RSC Advances

REVIEW

View Article Online
View Journal | View Issue

Cite this: *RSC Adv.*, 2024, **14**, 4666

Emerging tendencies for the nano-delivery of gambogic acid: a promising approach in oncotherapy

Sherif Ashraf Fahmy, †*[a] Rawan Elghanam,†[b] Gowhar Rashid,[c] Rana A. Youness[d] and Nada K. Sedky[e]

Received 23rd November 2023
Accepted 24th January 2024

DOI: 10.1039/d3ra08042k

rsc.li/rsc-advances

Despite the advancements in cancer therapies during the past few years, chemo/photo resistance, severe toxic effects, recurrence of metastatic tumors, and non-selective targeting remain incomprehensible. Thus, much effort has been spent exploring natural anticancer compounds endowed with biosafety and high effectiveness in cancer prevention and therapy. Gambogic acid (GA) is a promising natural compound in cancer therapy. It is the major xanthone component of the dry resin extracted from the *Garcinia hanburyi* Hook. f. tree. GA has significant antiproliferative effects on different types of cancer, and it exerts its anticancer activities through various pathways. Nonetheless, the clinical translation of GA has been hampered, partly due to its water insolubility, low bioavailability, poor pharmacokinetics, rapid plasma clearance, early degradation in blood circulation, and detrimental vascular irritation. Lately, procedures have been invented demonstrating the ability of nanoparticles to overcome the challenges associated with the clinical use of natural compounds both *in vitro* and *in vivo*. This review sheds light on the recent emerging trends for the nanodelivery of GA to cancer cells. To the best of our knowledge, no similar recent review described the different nanoformulations designed to improve the anticancer therapeutic activity and targeting ability of GA.

1. Introduction

Cancer is one of the prominent causes of death in both developing and wealthy countries, with a rapid growth in new incidence rates.[1] Existing chemotherapeutics, such as platinum-based drugs, antimetabolites, topoisomerase inhibitors, alkylating agents, anthracyclines, and protein kinase inhibitors, adopt specific direct or indirect pathways, which eventually inhibit the proliferation of tumor cells but habitually fail to eliminate cancer progression or avert its recurrence.[2–5] In addition to the serious systemic side effects, recurring treatment with chemotherapeutics ultimately results in the development of resistance by cancer cells against these drugs.[6] Hence, unveiling natural compounds that can preferentially impede cancer growth *via* stimulating apoptosis and target several cellular signaling pathways without developing resistance or causing toxic effects on healthy tissues is essential. Several natural compounds have been reported to exert compelling antitumor activities against various cancer cells through different mechanisms, such as inducing programmed cell death, halting angiogenesis, impeding inflammatory mediators, and initiating autophagic pathways.[7–11] The most prevalent groups of natural compounds with anticancer effects are polyphenols, phytochemicals, and xanthonoids.[12,13] Gambogic acid (GA) is the major xanthone component of the dry resin extracted from the *Garcinia hanburyi* Hook. f. tree.[14] It exhibits notable tumor-inhibiting effects on various tumors, including pancreatic, breast, lung, liver, gastric, and bone cancers. GA exerts its anti-tumor activities through different pathways, including restricting proteasome activity and regulating the development of tumor vascular endothelial cells to prevent the proliferation of cancer cells.[15] In addition, unlike conventional chemotherapeutics, GA possesses pleiotropic features that alter c-Jun N-terminal kinase-1 (JNK-1), nuclear factor-kappa B (NF-κB) and protein kinase B (AKT) signaling pathways.[15] Although being a promising asset in treating cancer and has granted the China Food and Drug Administration (CFDA) approval to enter Phase III clinical trials, GA has failed to pass the clinical superiority assessment owing to several limitations that thwart its clinical translation. These shortcomings include rigid structure, hydrophobicity, chemical

[a]*Department of Chemistry, School of Life and Medical Sciences, University of Hertfordshire Hosted by Global Academic Foundation, R5 New Garden City, New Capital, Cairo 11835, Egypt. E-mail: sheriffahmy@aucegypt.edu; Tel: +20 1222613344*

[b]*Nanotechnology Department, School of Sciences & Engineering, The American University in Cairo, AUC Avenue, P.O. Box 74, New Cairo, 11835, Egypt*

[c]*Amity Medical School, Amity University, Gurugram, Haryana, 122413, India*

[d]*Biology and Biochemistry Department, Molecular Genetics Research Team (MGRT), Faculty of Biotechnology, German International University (GIU), Cairo 11835, Egypt*

[e]*Department of Biochemistry, School of Life and Medical Sciences, University of Hertfordshire Hosted by Global Academic Foundation, R5 New Garden City, New Administrative Capital, Cairo, Egypt*

† Both authors contributed equally to this work.

instability, low bioavailability, poor pharmacokinetics, rapid plasma clearance, premature degradation in blood circulation, undesirable vascular inflammation, and a lack of selective targeting to the intended site of action.[16] Therefore, utilizing an unorthodox technology to address the challenges of using GA clinically is particularly crucial. A facile approach to solving the drawbacks of GA is to provide nano-delivery systems that can improve its hydrophilicity, bioavailability, and possibility of shielding GA from non-intended side reactions that cause its deactivation while simultaneously improving its targeting and uptake into the intended cancer cells.[17–19]

This review aims to comprehensively overview gambogic acid's chemical features, anticancer activities against different cancers, and the underlying anticancer mechanisms of action. In addition, we will discuss the nanodelivery systems recently employed for the nanoformulation of GA to address the challenges impeding its clinical translation while improving its anticancer potency and selective cancer cell uptake ability.

2. Gambogic acid's chemical characteristics

Gambogic acid (GA) is a natural compound with therapeutic properties, and its chemical formula is $C_{38}H_{44}O_8$, as illustrated in (Fig. 1).[14] GA, a naturally occurring prenylated xanthone derivative, is the most significant member of the xanthone family and is being studied for its potential use as a potent anticancer agent.[20,21] GA has been used in traditional Chinese medicine for centuries and has various biological properties, including anti-inflammatory, antioxidant, antiviral, and anti-infectious activities. In the past few years, several studies have reported its potent anticancer activities against broad types of cancer cells, as will be described in the following sections.[22,23] GA exhibits flash and boiling points of 251.4 °C and 808.9 °C and, respectively, and a pronounced maximum absorption wavelength of 365 nm.[24]

According to studies on the relationship between activity and structure, the 6-hydroxy and 3O-carboxy groups of the α,β-unsaturated ketone moiety from GA play a significant role in the biological activity of the compound. By covalently attaching to the active cysteine residues *via* Michael addition events, GA could also inhibit the activation of thioredoxin (TRX-1/2) proteins.[25,26]

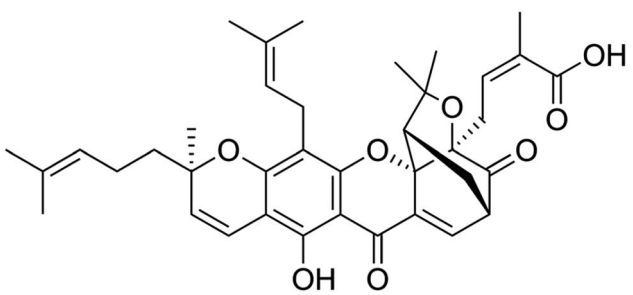

Fig. 1 Gambogic acid chemical structure.

3. Anticancer activities of gambogic acid

GA has superior anticancer activity when compared to other natural substances. Previous studies have shown that GA is a potent apoptosis inducer, anticancer drug, and tumor growth inhibitor. GA has been demonstrated to be a powerful natural drug with very low half-maximal inhibitory doses (IC50, nM range) against various cancer cell types.[14] Additionally, GA has been shown to have various anticancer properties, including the ability to suppress invasion, metastasis, and angiogenesis, as well as apoptosis, autophagy, and cell cycle arrest. GA shiwed a great potential in suppressing breast, pancreatic, prostate, lung, osteosarcoma, and other cancers adopting different mechanisms. Also, as mentioned above, GA can target c-Jun N-terminal kinase-1 (JNK-1), protein kinase B (AKT)/mammalian target of rapamycin (mTOR), AKT/forkhead box protein O1 (FOXO1)/BIM and nuclear factor kappa-B (NF-B).[20,21] In addition, GA can down-regulate heat shock protein (HSP90), and it is considered to be the heat-shock protein 90 (HSP90) inhibitor.[16,27]

3.1 Breast cancer

Breast cancer is the second most common cause of death for women and the most common malignancy to be detected. It is responsible for about one-fourth of all female cancers worldwide.[28] Although numerous chemotherapies that have been granted FDA approval are available, natural compounds have been shown to provide a safer alternative. As shown in Table 1, several studies have reported the anticancer activity of GA against breast cancer. GA was shown to increase SIRT1 expression *in vitro* to prevent the epithelial–mesenchymal transition in breast cancer cells. In addition, GA has been reported to reduce proliferation in human breast MDA-MB-231 cells, minimize tumor invasion and enhance SIRT1 mRNA and protein expression while repressing IL-6 production in MDA-MB-231 cells.[29] In another study on breast cancer, GA was shown to enhance the sensitivity of drug-resistant breast cancer cells to paclitaxel by modifying the sonic hedgehog (SHH) signaling route. However, as compared to either drug alone, the combination of both drugs has dramatically reduced the expression of SHH, GLI1, and PTCH1. Also, the combination of GA and paclitaxel led to markedly reduced tumor growth *in vivo* in mouse models and *in vitro*.[30]

3.2 Lung cancer

About 85% of lung cancer patients have non-small cell lung cancer (NSCLC), which is the most common cause of cancer-related death globally. The tumor suppressor liver kinase B1 (LKB1) controls polarity, growth, metabolism, and survival of cells. It is the most prevalent alteration in the NSCLC gene, also known as STK11; between 30% and 35% of NSCLC cases had mutant or inactive LKB1. The calcium/calmodulin kinase group includes the serine/threonine kinase LKB1. Individuals with wild-type LKB1 respond to chemotherapy differently from

Table 1 Gambogic acid for the treatment of different types of cancer

Cancer type	Cancer cell line	Mechanism of action	Remarks	Ref
Gastric signet ring cell carcinoma	SNU-16 cells	- Upregulated cleaved caspase 3, Bax, and cleaved PARP - Downregulated BCL-2	- GA had a dose-dependent antiproliferative effect - IC50 = 655.1 nm	33
Bile duct cancer, (cholangiocarcinoma)	KKU-M213 and HuCCA-1	- Inhibited Wnt/β-catenin signaling pathway - Induced ER stress - Induced apoptosis	- Potent cytotoxicity - Inhibited cell proliferation	35
Liver cancer (human hepatocellular carcinoma)	HepG2, and SMMC-7721)	- Targeted thioredoxin reductase (TrxR) - Induced apoptosis	- Synergistic cytotoxic effect with hydrogen peroxide sheds	36
Colon cancer	SW620 cell line	- Altered the expression of PI3K, AKT, phosphorylated-AKT, P21 and MMP-2 and -9	- Inhibited cell proliferation in a dose-dependent manner	39
Colon cancer	HT-29 cell line	- Worked on mitochondrial pathways	- Inhibited cell proliferation - Exhibited a dose-dependent inhibition of growth in a mouse xenograft model - Induced apoptosis	40
Colorectal cancer	HT-29 cell line	- Decreased miR-21 expression - Blocked PI3K/Akt	- Inhibited cancer cell proliferation, invasion, and migration - Increased phosphatase and tensin homolog activation - Induced apoptosis	41
Breast cancer	MCF-7 cells	- Inhibited the expression of SIRT1 - Increased the expression of p27Kip1	- Reduced cell proliferation - Triggered cell apoptosis - Promoted the production of ROS	42

patients with mutant LKB1 who have non-small cell lung cancer. GA was found to increase the sensitivity of NSCLC cells harboring LKB1 *in vivo* and *in vitro*. In the presence of LKB1, which is implicated in the augmentation of p-AMPK, the selective inhibition of mTOR signaling provides a higher suppression of NSCLC. GA-enhanced E-cadherin cooperates with LKB1, resulting in the up-regulation of p-AMPK and consequent blockage of the mTOR signaling pathway.[31]

3.3 Stomach cancer

Among all cancers, gastric cancer is ranked the fifth in the world. Finding novel treatments for advancing stomach cancer treatment is critically needed, as it is one of the leading causes of cancer death globally. Several studies have shown that GA has anticancer potential against stomach cancer. GA blocked the circRNA_ASAP2/miR-33a-5p/CDK7 to prevent the spread of gastric cancer. The expression level circ_ASAP2 in gastric cancer tissues was more significant than in normal gastric tissues. After GA treatment, circ_ASAP2 was downregulated. Compared to normal cells, GA downregulated CDK7, with higher levels of MiR-33a-5p expression and reduced CDK7 protein expression. Also, miR-33a-5p was linked to CDK7, and circ_ASAP2 served as a sponge for miR-33a-5p.[32] In addition, it was revealed that GA inhibits the proliferation of stomach cancer cells by upregulating apoptotic proteins such as cleaved caspase 3, Bax, and cleaved PARP, while downregulating BCL-2, an anti-apoptotic protein. Additionally, the administration of GA increased levels of LC3, an autophagy marker, as well as 8-oxo-dG, a widely recognized biomarker that leads to oxidative damage to cancer DNA. Thus, the capacity of GA to promote apoptosis and autophagy is thought to be the cause of its antiproliferative action against cancer cells.[33]

3.4 Liver cancer

Hepatocellular carcinoma (HCC) and cholangiocarcinoma (CCA) are the two histological kinds of primary hepatic malignancy, also referred to as liver cancer. The most common form of liver cancer worldwide is HCC.[34] More than 80% of all identified primary liver cancers in Thailand are of the most frequent pathogenic kind, known as cholangiocarcinoma (CCA). Due to its aggressiveness and the generally dismal prognosis for individuals with this disease, CCA is still linked to high fatality rates, especially in northeast Thailand. Most CCA patients are now treated with chemotherapy, with only around a quarter of patients being suitable for surgical tumor removal. Unfortunately, despite exploiting several tolerance mechanisms, CCA cannot withstand regular treatment. Therefore, finding a novel medication with high efficacy for treating CCA is crucial.[34] GA

Table 2 Combination therapy of chemotherapeutic drugs with GA

Chemotherapeutic drug	Cancer type	Cancer cell line	Mechanism of action	Remarks	Ref
Gemcitabine	Non-small cell lung cancer	**A549 and NCI-H1299 cell lines**	- Reduced angiogenesis - Modified MAPK/ERK, PI3K/AKT, and NF-B	**IC50 = 185 nM**	14
Docetaxel	**Breast cancer**	**MCF-7 cell line**	**- Inhibited P-gp**	**IC50 = 1.43 ± 0.14 μM**	47
Paclitaxel	**Triple-negative breast cancer**	**MDA-MB-231 and MDA-MB-468 MDA-MB-231 and MDA-MB-468**	**- Worked on the SHH signaling pathway**	**- Increased the sensitivity**	30
Docetaxel	Gastrointestinal cancer	**BGC-823, MKN-28, LOVO, and SW-116 cell lines**	- Worked on β-tubulin III, tau, and survivin	- Reduced the mRNA expression of docetaxel genes	43
Chloroquine	Pancreatic cancer	**PANC-1 and BxPC-3 cell lines**	- Increased ROS production - Increased the expression of LC3-II and Beclin-1	- Induced cytoprotective autophagy	44
Cisplatin	Non-small-cell lung cancer	**A549, NCI-H460, and NCI-H1299 cell lines**	- Inhibited NF-B and MAPK/HO-1	- Synergistic action - Sensitized cancer cells	45
5-Fluorouracil	Colorectal cancer	**SW480 and HCT116 cell line**	- Decreased P53, survivin and thymidylate synthase (TS) mRNA and protein levels	**5-FU IC50 = 122.14 μM**	48
5-Fluorouracil	**Nasopharyngeal carcinoma**	**Human NPC cell lines including CNE-1, CNE-2, 5–8F, 6–10B and the HNEpC**	- Induced apoptosis, the **- Regulated the genes of IKBKB, STAT3, GRB2, CASP3, STAT1, CASP8, BCL2, EGFR, STAT5B**	**GA + 5-FU IC50 = 8.11 μM IC50 < 10 μM**	49
Retinoic acid chlorochalcone	Osteosarcoma	**MG63 cell line**	- Increased apoptosis - Inhibited proliferation	**- GA IC50 = 0.89 μg mL^{-1} combination therapy IC50 = 0.35 μg mL**	50
Imatinib	Myeloid leukemia	**KBM5, KBM5-T315I, and K562 cell lines**	- Inhibited the proteasome - Induced apoptosis - Downregulated caspase-dependent Bcr-Abl	- Sensitized cancer cells - Induced cell proliferation	46
Irinotecan	Liver cancer	**Huh7 and HepG2 cell lines**	- Decreased CES1 and CES2 by activating ERK and p38 MAPK	- Had a concentration and time dependent effect - Hydrolytic activity decreased	51
Gefitinib	Non-small-cell lung cancer	**NCI-H1975 cell line**	- Reduced AKT, MEK1/2 and ERK1/2 - Increased expression of Bax/Bcl-2	- Enhanced apoptotic effect	52
NaI131	**Non-small-cell lung cancer**	**NSCLC A549 cell line and the drug-resistant A549/cisplatin and A549/Taxol cell lines**	**- Decreased protein levels of CDK1, cyclin B, mtp53, HSP90, Bcl-2 and P-gp** **- Increased protein levels of Bax** **- Decreased mRNA levels of p53 and HSP90**	**- Sensitizer** **- Reduced drug-resistance**	53

was found to cause cell cycle arrest at the G0/G1 phase, reduce HCC and CCA cell proliferation, and trigger apoptosis *via* the mitochondria-dependent and extrinsic death receptor pathways.[34] In CCA cells, GA demonstrated potent cytotoxicity accompanied by a considerable reduction in cell proliferation, the promotion of G1 arrest, and activation of caspase 3 mediated death. GA inhibited the expression of c-Myc, a downstream target gene of Wnt/-catenin signaling, and attenuated -catenin transcriptional and protein levels. In KKU-M213, GA activated ER stress-related genes, increasing CCA's sensitivity to gemcitabine.[35] In HCC of SMMC-7721 cells, it was found that GA targets thioredoxin reductase (TrxR) to cause oxidative stress, which in turn might lead to the induction of apoptosis. GA predominantly targets the selenocysteine residue to block the Trx-reduction activity of the antioxidant enzyme TrxR1. This causes a buildup of reactive oxygen species and the breakdown of the intracellular redox equilibrium.[36]

3.5 Colon cancer

Colorectal cancer is the third most frequent and deadly cancer globally. Most colorectal cancer patients are diagnosed at an advanced stage because of the lack of early symptoms a study

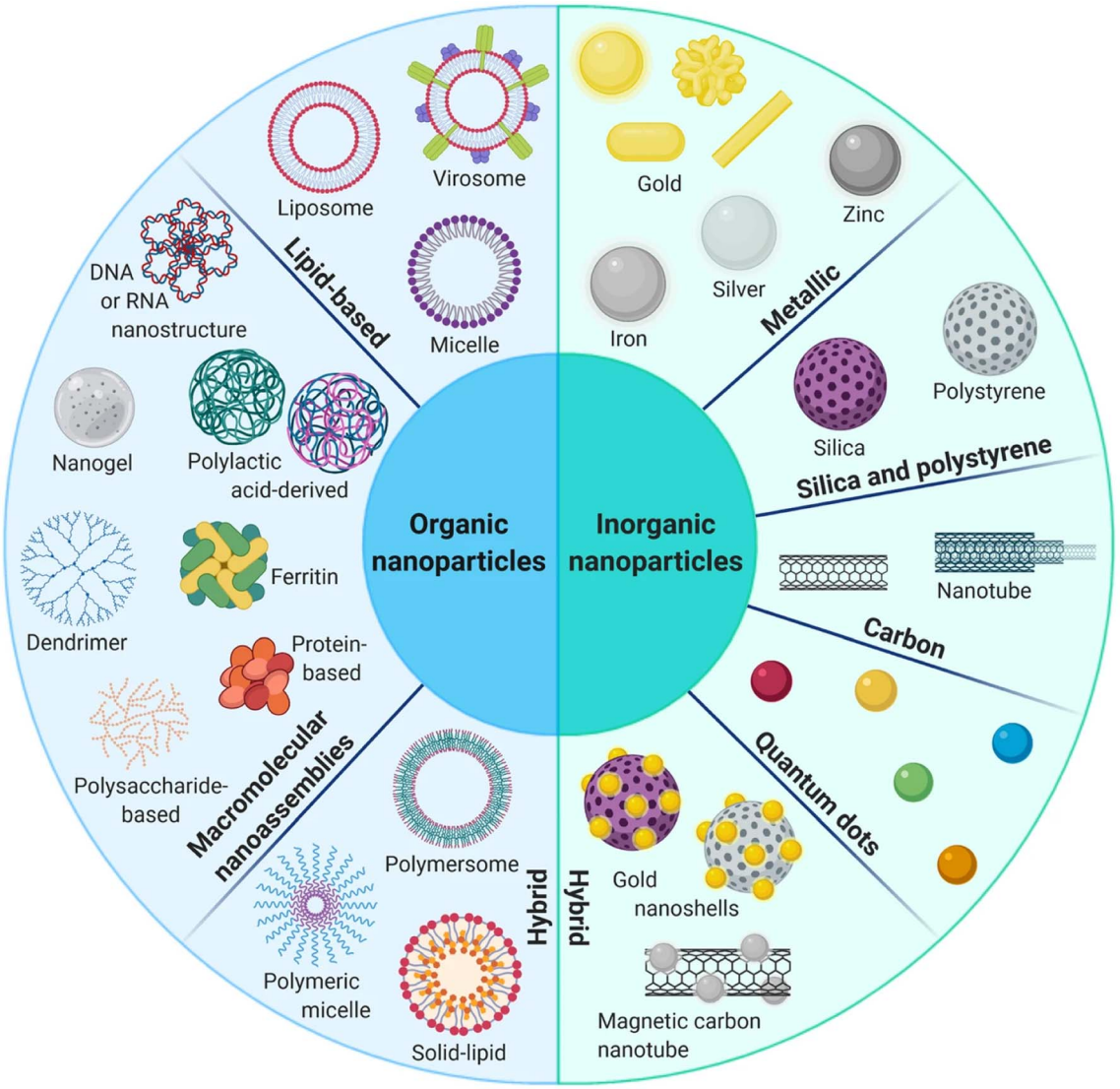

Fig. 2 Schematic diagram representing the organic, inorganic and hybrid NPs. This figure has been reproduced from ref. 55 with permission from Springer, copyright 2021.

found that GA reduces the viability of colorectal cancer cell lines, HCT116 and CT26, in a dose-dependent manner. GA induced colorectal cancer cell pyroptosis *via* the gasdermin E (GSDME)-a dependent pathway and triggered an antitumor immune response. GA creates pores and giant bubbles in the cancer cell membrane, causing pyroptosis, a type of programmed cell death that significantly affects the immune response against tumors. In addition, GA causes GSDME breakage and simultaneous caspase-3 activation. Furthermore, GA triggered an immune response *via* increasing the production of dendritic cells, cytotoxic T lymphocytes, CD3+ T cells, and effector memory T cells.[37] GA treated colorectal cancer by its effect on the expression of miR-199a-3p. The miR-199a-3p hinders the development and spread of several cancerous tumors. Expression of miR-199a-3p was found in normal human colon epithelial cells and human colorectal cancer cell strain SW480. SW480 had statistically lower miR-199a-3p than normal cells. The expression of miR-199a-3p in cancerous cells following GA treatment was considerably more significant than in cancerous cells not receiving GA treatment. The miR-199a-3p group showed increased apoptosis and decreased proliferation and invasion ability after treatment of GA in SW480, whereas the group that received the miR-199a-3p inhibitor showed the opposite effects. Thus, GA can treat colorectal cancer by enhancing the expression of miR-199a-3p.[38] In another study, the mechanism of GA on human colon cancer SW620 cells was identified. The relative protein expression levels of phosphoinositide 3-kinase (PI3K), protein kinase B (AKT), P21, and matrix metalloprotease (MMP)-2 and -9 between different concentrations of GA were examined by Western blotting. GA with low, middle, and high concentrations decreased SW620 cell growth, invasion, and migration compared to the untreated groups. Additionally, there were notable variations in migration, invasion, and proliferation between groups that received

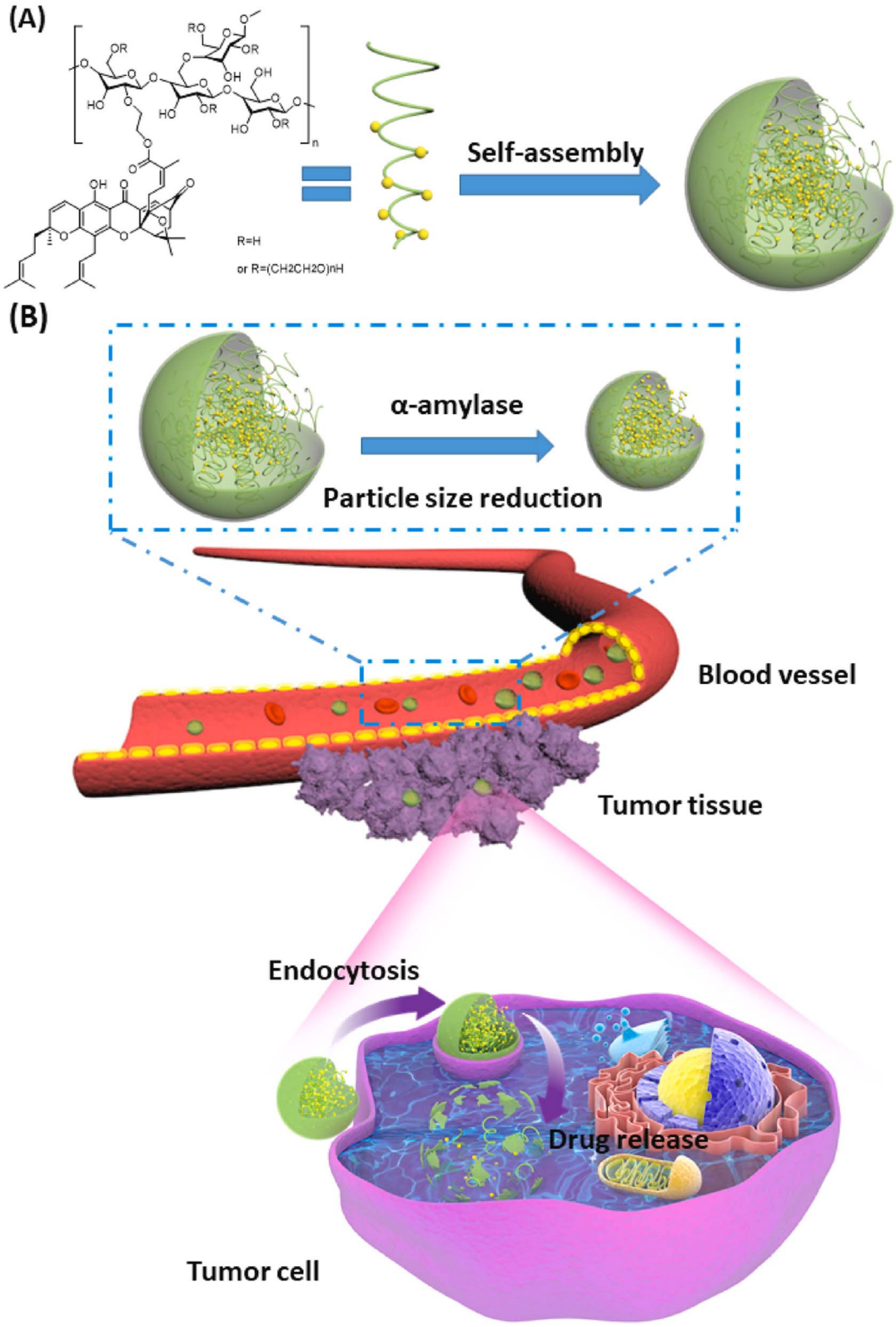

Fig. 3 Schematic diagram illustrating (A) the self-assembly of GA/HES to form GA-HES/NPs and (B) further size reduction by systemic α-amylase, followed by tumor cellar uptake *via* endocytosis and EPR effect. This figure has been reproduced from ref. 68 with permission from Elsevier, copyright 2022.

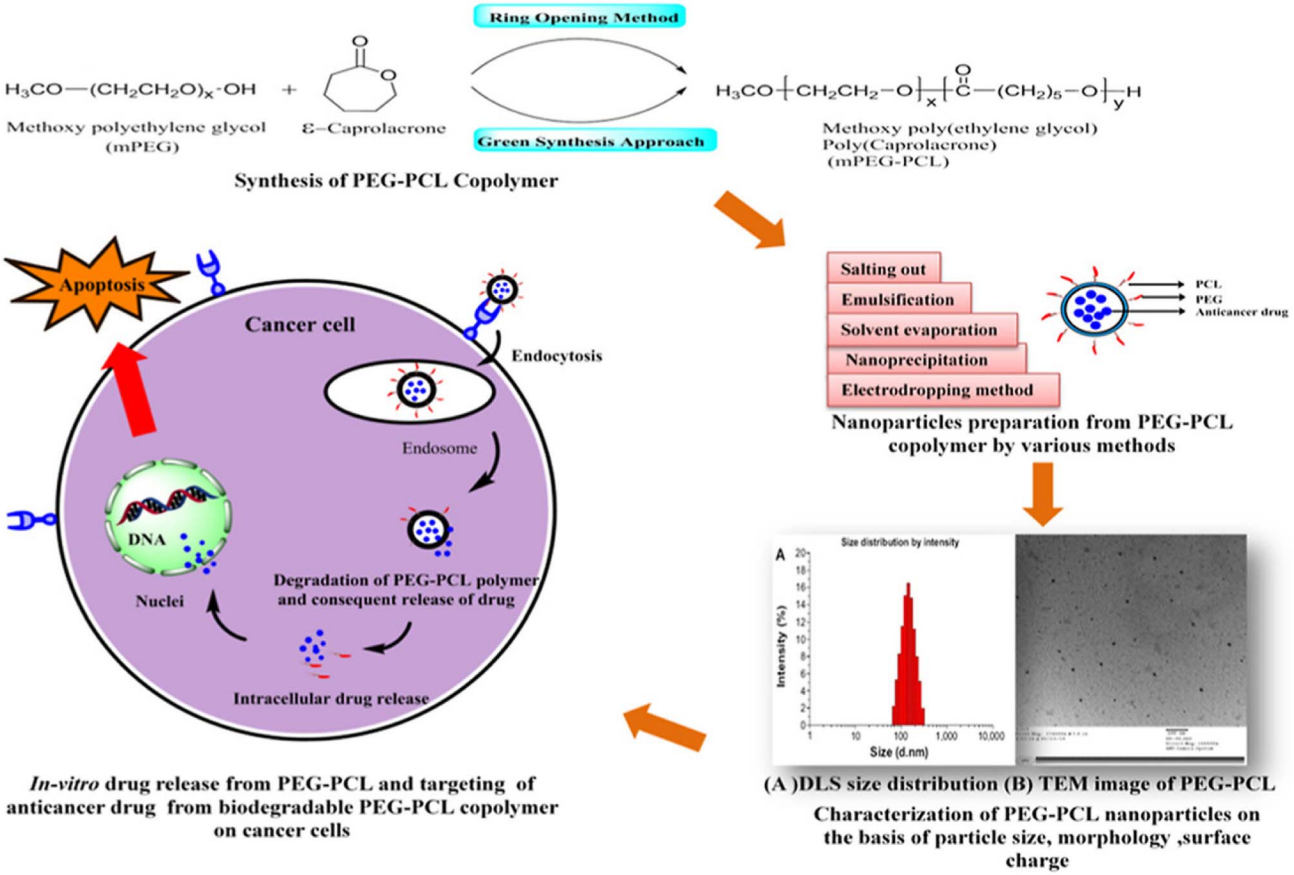

Fig. 4 Schematic diagram demonstrating the chemical synthesis of PEG-PCL copolymers, their nanoformulation, and intracellular uptake into cancer cells. This figure has been reproduced from ref. 66 with permission from Elsevier, copyright 2020.

various concentrations of GA. After treatment with GA, there were dose-dependently significant changes in the expression levels of PI3K, AKT, phosphorylated-AKT, P21, MMP-2, and -9 compared to the untreated group. Thus, GA inhibited the proliferation and spread of colon cancer in a dose-dependent manner, possibly *via* a pathway dependent on PI3K/AKT/P21/MMP-2/9.[39]

4. Combination therapy of chemotherapeutic drugs with GA

Chemotherapeutic drugs were combined with GA to increase chemo-sensitization or give a synergistic effect to overcome chemotherapy drug resistance. GA chemo-sensitizes cancer by regulating numerous signaling pathways, including MAPK/ERK, PI3K/AKT, and NF-B. Thus, GA has attracted interest as a cancer-fighting drug in combination therapies. The chemotherapeutics used in conjunction with GA to treat different types of cancers with different mechanisms are illustrated in (Table 2). GA has shown to raise the intracellular concentration of chemotherapeutics in cancerous cells. Several chemotherapeutics such as Gemcitabine, Docetaxel, Chloroquine, Cisplatin, 5-Fluorouracil, Retinoic acid chlorochalcone, Imatinib, Irinotecan, and Gefitinib were used in combination with GA.

For instance, GA was used in combination with docetaxel against several gastrointestinal cancer cells, such as BGC-823, MKN-28, LOVO, and SW-116 cell lines, using the MTT test. GA had a synergistic effect, enhanced cytotoxic and apoptotic effects in all cell lines. GA also significantly reduced the mRNA expression of genes associated with the administration of docetaxel, such as tau, β-tubulin III, and survivin, in BGC-823 cells. Thus, combinatorial therapies could provide potential anticancer effects against gastric and colorectal malignancies because they exhibit a synergistic antitumor effect.[43] Apoptosis and cell viability of chloroquine and GA against pancreatic cancer were assessed. The effectiveness of GA and chloroquine was evaluated on a xenograft tumor model of pancreatic cancer. In pancreatic cancer cells, GA increased the expression of the proteins LC3-II and Beclin-1 while decreasing the expression of P62. GA also boosted autophagic flow and the production of acidic vesicular organelles, including autophagosomes. So, the autophagic process was stimulated by GA. In addition, GA increased ROS formation and decreased the mitochondrial membrane's potential, both of which helped to activate autophagy. Chloroquine's suppression of autophagy further decreased the mitochondrial membrane's potential and accelerated ROS buildup. GA and chloroquine effectively slowed the tumor's growth in the xenograft tumor model. Hence,

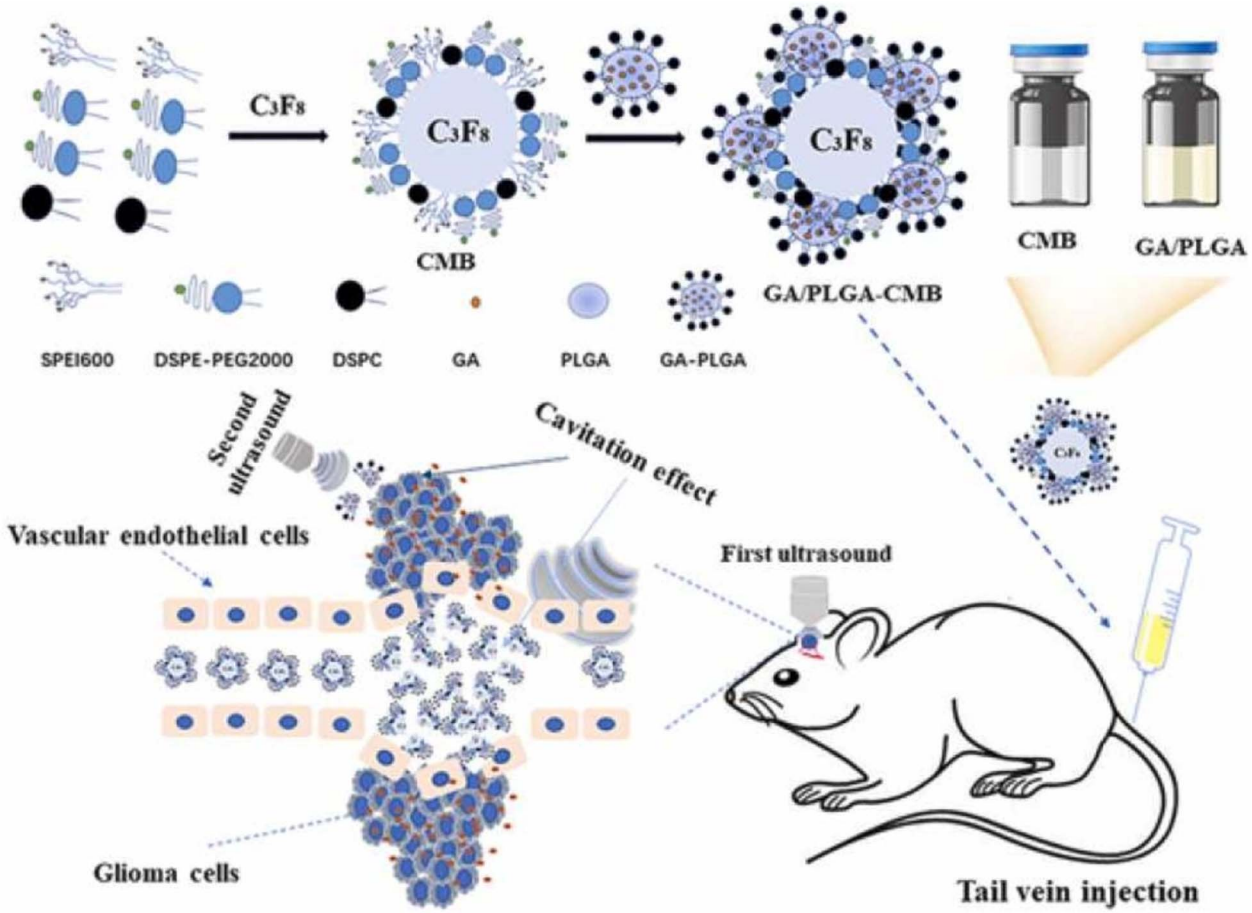

Fig. 5 Formulation of ultrasound-triggered GA-loaded nanobubble-microbubble (PLGA–CMB) complexes for effective glioma treatment. This figure has been reproduced from reproduced from ref. 70 with permission from Elsevier, copyright 2022.

pancreatic cancer cells undergo cytoprotective autophagy when exposed to GA. The suppression of autophagy enhances GA's cytotoxicity because it causes more reactive oxygen species (ROS) to accumulate in tumor cells.[44] When GA was used in combination with cisplatin, it had a synergistic effect in the non-small-cell lung cancer (NSCLC) treatment. The cell viability test showed that the combination therapy significantly synergized the A549, NCI-H460, and NCI-H1299 cell lines. Boosted sub-G1 phase cells and improved PARP cleavage showed that, when compared to other treatments, the combination therapy dramatically boosted apoptosis. Additionally, in A549 and NCI-H460 cell lines, the combination therapy improved caspase-3, -8, and 9 activation, raised the expression of Fas and Bax, and lowered the expression of Bcl-2, survivin, and X-inhibitor of apoptosis protein (X-IAP). Additionally, there was a correlation between elevated reactive oxygen species formation and increased apoptosis. Additionally, it was discovered that GA might block the signaling pathways for NF-B and mitogen-activated protein kinase (MAPK)/heme oxygenase-1 (HO-1) that have been shown to diminish ROS emission and impart cisplatin resistance after cisplatin therapy. These findings showed that the combination therapy boosted the antitumor effects on A549 xenograft models by suppressing NF-B and HO-1, leading to the induction of apoptosis. Hence, through the inactivation of the NF-B and MAPK/HO-1 signaling pathways, GA sensitized lung cancer cells to cisplatin *in vitro* and *in vivo*.[45] GA was used in combination with Imatinib for the treatment of Myeloid leukemia. GA decreased imatinib-resistant Bcr-Abl-T315I xenograft growth in nude mice and caused apoptosis and cell proliferation inhibition in Myeloid leukemia cells *via* stimulating caspase activation. Thus, GA could overcome the imatinib resistance and increase its sensitivity towards Myeloid leukemia by boosting Bcr-Abl downregulation.[46]

5. Gambogic acid nano-delivery using nano-particulates

Nanodelivery systems have emerged as a revolutionary approach to address the challenges associated with the clinical translation of GA and to advance its druggability, as mentioned above, such as low water solubility, poor pharmacokinetic profiles, premature biodegradation in the bloodstream causing short half-life, vascular inflammation and non-selective targeting to cancer tissues. Nanodelivery systems are classified into organic, inorganic, and hybrid nanoparticles (NPs), as illustrated in Fig. 2. Organic NPs, such as macromolecular assemblies and lipid-based NPs. Yet characterized by low stability, organic NPs are biocompatible and biodegradable, and their

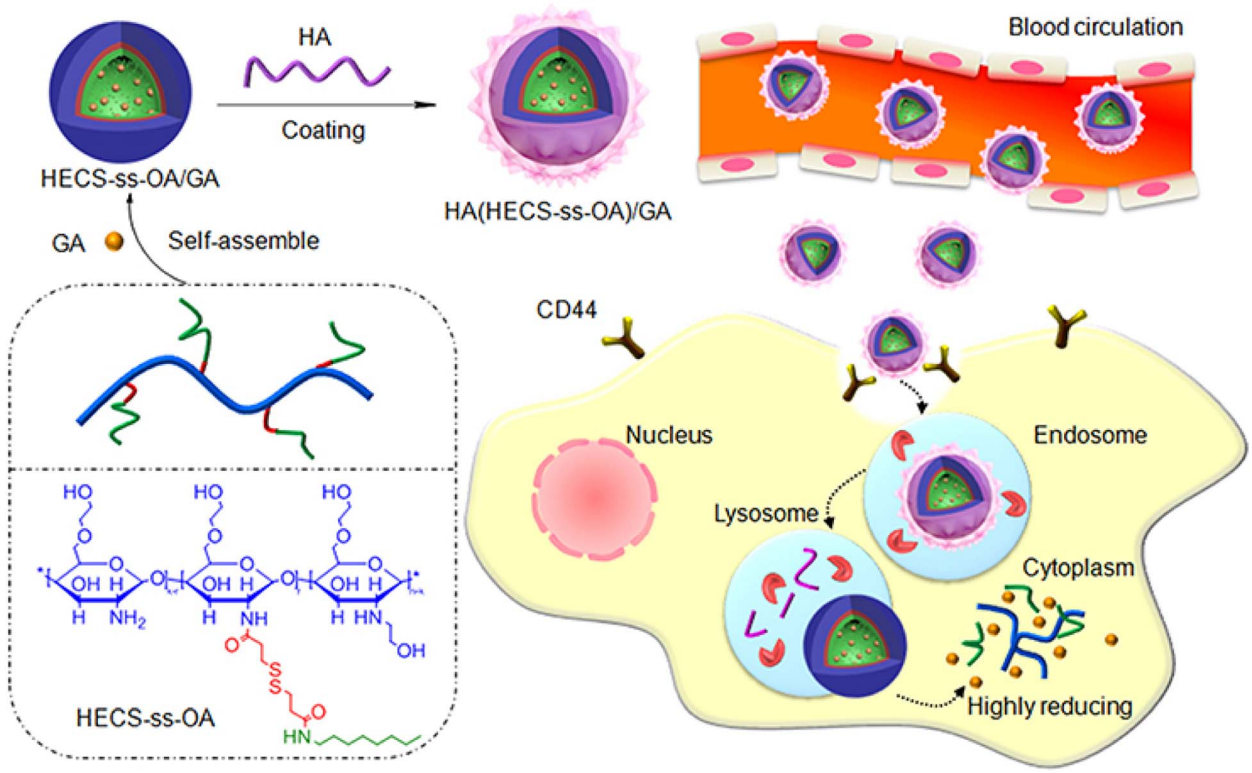

Fig. 6 A schematic diagram illustrating the design of HA(HECS-ss-OA)/GA *via* self-assembly and the mechanism of cancer cells' internalization and redox-triggered release of GA. This figure has been reproduced from ref. 71 with permission from Taylor & Francis, copyright 2019.

surfaces could be decorated with various targeting functional groups. Inorganic nanoparticles, such as silica, metallic, magnetic NPs, carbon nanotubes, and quantum dots, are characterized by unique optical properties and electronic features while maintaining high stability, making them the best candidates for theranostics. However, inorganic NPs suffer

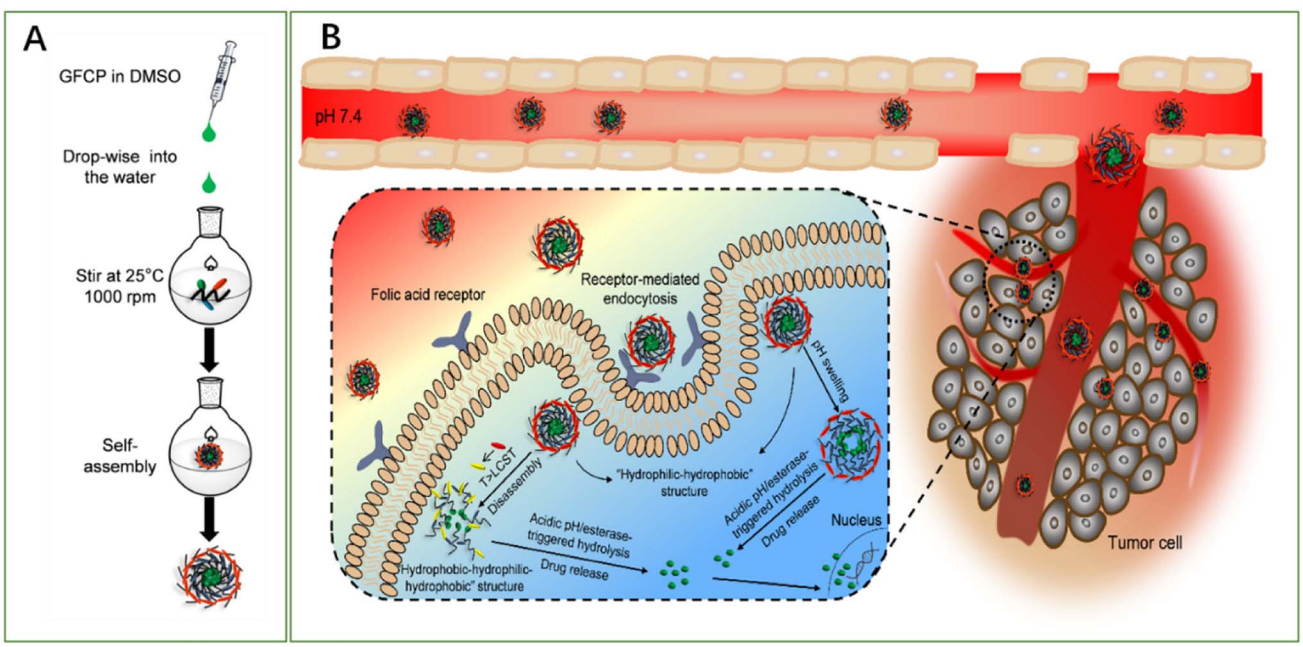

Fig. 7 Schematic diagram representing (A) the methodology utilized for micelles fabrication and (B) the mechanism by which the micelles deliver GA into cancer cells, boosting its anticancer effect. This figure has been reproduced from ref. 72 with permission from Elsevier, copyright 2021.

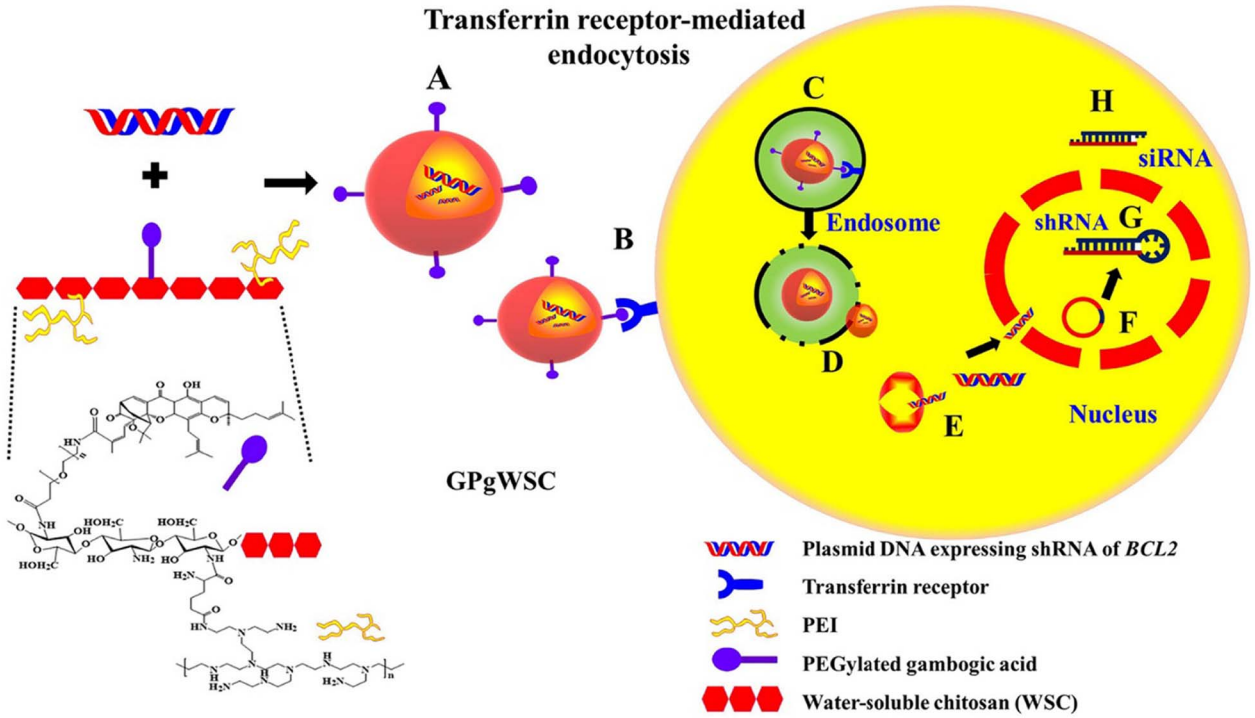

Fig. 8 Schematic diagram illustrating (A) the synthesis of nanopolyplexes grafted with GA and pDNA (BCL2 shRNA-expressing vector, psiRNA-BCL2), (B) the ability of the polyplexes to bind the overexpressed transferrin receptors found on the surface of human colon HCT116 cancer cells, (C) endosomal formation, (D) proton sponge effect leading to endosomal diversion, (E) dismantle of nanopolyplexes releasing pDNA into HCT116 cells, (F) nucleus localization through nuclear pores, (G) anti-*bcl-2* shRNA expression, (H) siRNA processing through *bcl-2* mRNA silencing. This figure has been reproduced from ref. 65 with permission from Elsevier, copyright 2022.

from being low biodegradable. Thus, hybrid NPs were developed to integrate the advantages of organic and inorganic NPs, aiming at improving biodegradability, biocompatibility, stability, and targeting abilities.[54–58] Nanodelivery systems have been extensively studied for cancer-targeted therapies owing to their extraordinary abilities to advance cancer therapeutics by prolonging circulation time, improving bioavailability, and water solubility while reducing undesirable adverse effects. In addition, the NPs can preferentially accumulate into malignant cells *via* passive targeting achieved by the enhanced permeability and retention (EPR) effect.[59–61] On the other hand, using NPs in clinics is still challenging due to the congested invention process and multifaceted drug pharmacokinetics and pharmacodynamics in the body. Moreover, the NPs that involve physical interactions to incorporate therapeutics agents might suffer from drug leakage, resulting in low drug loading and encapsulation efficiencies.[62–64] In the following sections, we will discuss the recent studies involving the use of different organic and inorganic NPs for the nanoformulation of GA, in an attempt to overcome the obstacles that hinder its application.

5.1 Polymeric nanoparticulates

5.1.1 Polymeric nanoparticles. Synthetic ((poly(lactide), poly(caprolactone), poly(lactide-*co*-glycolide) copolymer, and poly(acrylates)) and natural (chitosan, pectin, and albumin) polymers are widely used to design polymeric NPs owing to their biocompatibility and biodegradability. Two primary approaches are commonly used to create polymeric NPs: the "top-down" and the "bottom-up" approaches. The desired NPs can be produced using a variety of techniques, including solvent evaporation, nanoprecipitation, and interfacial polymerization.[65–67]

In one study, GA was linked with poly(ethylene glycol) monomethyl ether (mPEG) polymer using two different sensitive linkages, valine–citrulline (VC) and cystamine forming NPs with an average particle size of 148.3 ± 3.21 nm and a PDI of 0.190 ± 0.036. The designed nanosystem was shown to overcome the GA limitations by increasing its water solubility and enhancing its selective release in the acidic cancerous microenvironment. In addition, the albumin adsorption assay showed that the designed NPs had diminutive binding to albumin, demonstrating their circulation endurance. Moreover, NPs showed remarkable cytotoxicity against HepG2 liver cancer cells with minimum toxicity against normal ones. The NPs exerted their anticancer effects by inhibiting the G0/G1 phase proliferation and triggering early and late apoptosis.[67]

Another study involved the use of hydroxyethyl starch (HES), a carbohydrate polymer with superior hydrophilicity, biocompatibility, and biodegradability, for encapsulating GA. HES modified the chemical structure of GA, creating amphiphilic molecules that can self-assemble in the aqueous medium to form GA-HES/NPs, as presented in Fig. 3. The produced NPs had a size of 174 nm with a PDI of 0.094 and a zeta potential value of

Table 3 Polymeric NPs loaded with GA for cancer therapy

Polymeric nanocarrier	Co-loaded drug/coatings/ functionalized)	Preparation method	Physicochemical characteristics	Cancer cell line	Ref.
Poly(lactic-*co*-glycolic acid)	Colon cancer cell membrane	Emulsification method	Size = 182 nm EE% = 85.5 ± 4.6% DL = 29.9 ± 0.8%	CT26 colon cancer	73
PEG-PLA NPs	Erythrocyte membrane (RBCm) coat	—	Size = 102.3 ± 3.1 nm PDI = 0.15 EE = 79.11 ± 1.42%	HepG2 hepatocellular carcinoma	74
PLGA	Erythrocyte membrane (RBCm) coat	Lipid insertion method	Size = 153 ± 3.83 nm	Caco-2, HT-29, and SW480 Colorectal cancer	75
Chitosan	—	Nanop recipitation	Size = 83.4 nm& 78.8 nm PDI = 0.183& 0.207 ZP = 12.3 ± 1.1 mV&13.1 ± 1.2 Mv	MB49 and NIH-3 T3 bladder cancer	76
Chitosan	Hyaluronic acid	—	Size = 210 nm ZP = +20 mV DL% = 18%	A549 cells	71
Chitosan	Folic acid/poly-*N*-isopropylacrylamide	Nano-precipitation method	Size = 87.5 ± 1.91 nm ZP = −8.12 ± 1.01 mV DL% = 21.05 ± 0.46%	MCF-7, HepG2, LO2, and HeLa cells	72
Chitosan	Polyethylenimine (PEI)	—	—	HCT116, LoVo, and MCF-7 cell lines	65
PEG	Linkages, valine–citrulline, and cystamine	—	Size = 148.3 ± 3.21 nm PDI = 0.190 ± 0.036	HepG2 Liver cancer	67
Hydroxyethyl starch	—	Nano precipitation	Size = 174 nm PDI = 0.094 ZP = −5.55 ± 0.56 mV	4T1 cells mouse breast cancer cells	68
PEG-PCL	—	Single emulsion method	Size = 143.78 nm EE% = 81.3%, DL% = 14.8%	Gastric cancer	69
Poly(lactic-*co*-glycolic acid) (PLGA)	Lipid microbubbles	W/O/W double emulsion method	Size = 869.7 ± 79.50 nm ZP = 7.22 ± 1.87 mV	U87 or U251 cells Glioma (brain tumor)	70

(ZP) of −5.55 ± 0.56 mV. The synthesized GA-HES/NPs are characterized by prolonged systemic circulation and a gradual decline in size after entering the bloodstream owing to the presence of α-amylase, enhancing their penetration and massive accumulation inside malignant cells (Fig. 3). Moreover, GA-HES/NPs could be passively targeted into cancer cells through the EPR effect, where, under the acidic conditions of cancer microenvironments, free GA will be selectively released and exert its anticancer effects. Thus, GA-HES/NPs had a specific capacity for tumor targeting and deep tumor penetration, which could improve GA's therapeutic efficacy for cancer treatment.[68]

The diblock poly(ethylene glycol)methyl ether-*block*-poly(ε-caprolactone) copolymers (PEG-PCL) are another advantageous biomedical polymeric material because of their facile synthesis, amphiphilic nature, biodegradability, biocompatibility, and ability to achieve a sustained release behavior. This distinctive quality has prompted their relevance, particularly in administering anticancer drugs through diverse nano-aggregates such as micelles, nanogels, microspheres, and nanospheres.[66] The PEG-PCL copolymers are synthesized by chemical (ring-opening) or green approaches. Then, the PEG-PCL NPs loaded with different anticancer agents are prepared using different methods, including salting out, emulsification, solvent evaporation, nanoprecipitation, or electrodropping. The designed NPs using one of these methods exhibited nanosizes and spherical morphologies. The prepared PEG-PCL NPs could be entrapped into tumor cells *via* endocytosis, where they are degraded and intracellularly release their cargos under acidic conditions in cancer cells, exerting their anticancer effects (Fig. 4). In order to provide efficient anticancer drug delivery systems and regulated drug release profiles, a wide range of anticancer medicines and bioactive have been encapsulated in PEG-PCL copolymers. PEG-PCL copolymer-based nanoparticles have made significant strides recently as anticancer drug delivery vehicles thanks to their increased hydrophobic drug loading capacities, improved bioavailability, resistance to phagocyte overpowering, reduced blasted discharge, and also in increasing the scattering time of drug within the bloodstream during systemic inoculation.[66]

For instance, GA was loaded into PEG-PCL NPs were fabricated and exhibited an average size of 143.78 nm, encapsulation efficiency of 81.3%, and loading capacity of 14.8%. The NPs also displayed excellent stability, strong biocompatibility, and a prolonged release profile. The *in vitro* uptake assessment showed that the NPs were efficiently uptaken into gastric cancer cells through endocytosis in a time-dependent behavior compared to unloaded GA. The *in vivo* findings showed that the formulated NPs successfully exhibited a potent antiproliferative activity against gastric cancer cells with negligible toxic effects

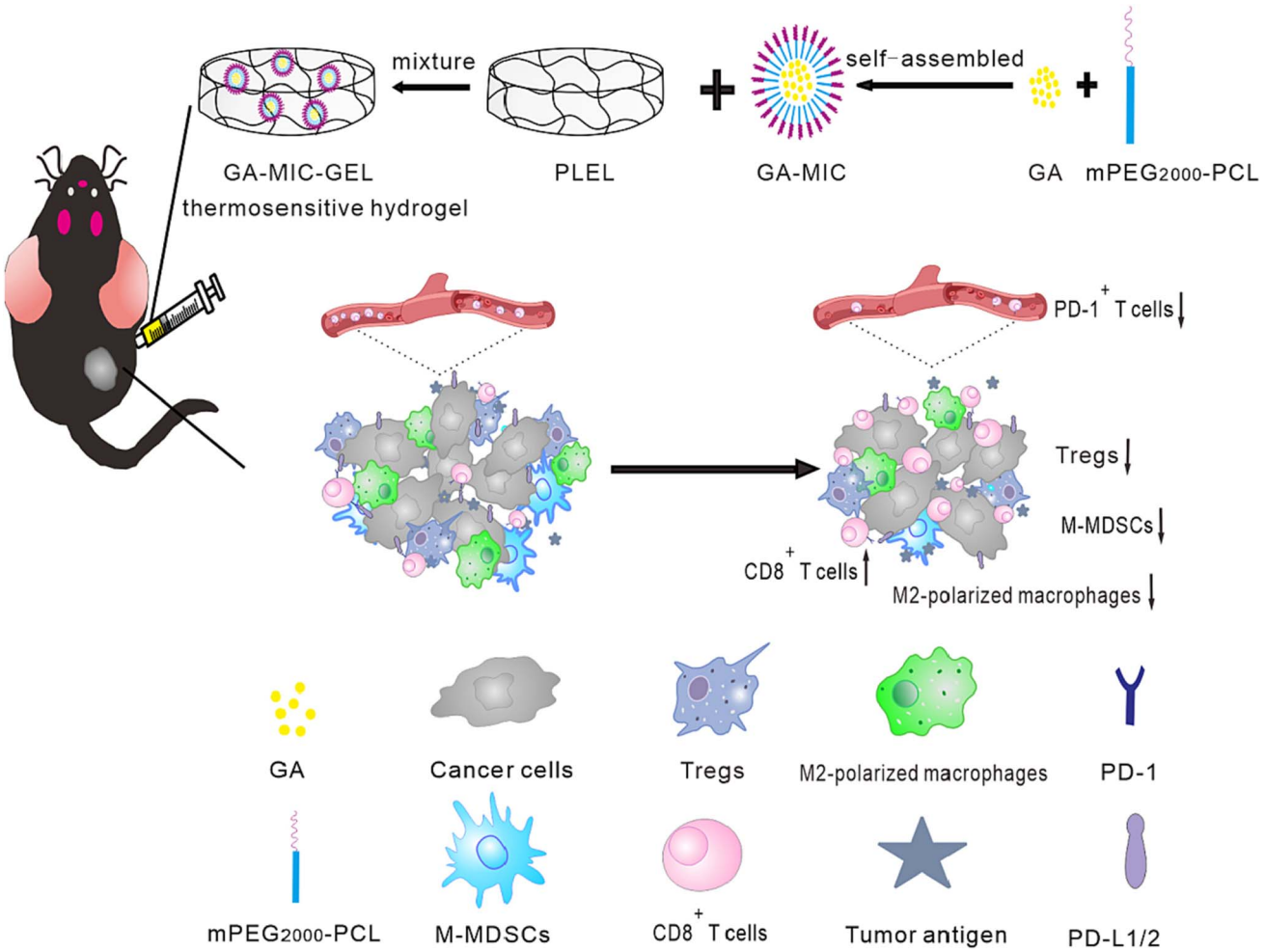

Fig. 9 Schematic representation of the prepared thermosensitive hydrogel comprising GA micelles with improved anticancer activities and enhanced antimalignancy immune activation. This figure has been reproduced from ref. 78 with permission from Elsevier, copyright 2022.

on other tissues owing to the downregulation of the cysteine proteases 3 precursor (pro-caspase3).[69]

Using GA as a potential anticancer agent in brain cancer is challenging due to its low bioavailability and poor permeability across the blood–brain barrier (BBB). Thus, a recent study nanoformulated GA into ultra-sound triggered anionic poly(-lactic-*co*-glycolic acid (PLGA) nanobubbles conjugated onto cationic lipid microbubbles (CMBs), formed of 1,2-distearoyl-*sn*-glycero-3-phosphocholine (DSPC), *N*-[methoxy (polyethylene glycol)-2000] (DSPE-PEG2000) and polyethyleneimine (PEI), through electrostatic interactions for effective treatment of glioma. The resulting GA/PLGA–CMB had a high drug encapsulation capacity of 96.81% ± 1.63%, drug loading of 7.75% ± 0.13%, and outstanding contrast imaging capacity. The prepared NPs were vein-injected into mice and exposed to low-intensity focused ultrasound (FUS). This triggered the first cavitation in GA/PLGA–CMBs, which opened BBB and released GA/PLGA to the glioma area by improving GA transport into the brain. Afterwards, upon the second exposure to FUS, GA/PLGA cavitation took place once more, which boosted the access of GA into cancer cells and substantially hampered the expansion of glioma. Thus, this tactic provided a promising stimulus-responsive delivery system for the controlled delivery of GA into the brain (Fig. 5).[70]

Another study has reported the formulation of hyaluronic acid (HA)-coated redox-sensitive chitosan-based (*O*,*N*-hydroxyethyl chitosan-octylamine) NPs, HA(HECS-ss-OA)/GA, *via* self-assembly for the targeted cytoplasmic delivery of GA into lung cancer cells (A549) (Fig. 6). The decoration of the chitosan NPs with HA has facilitated the effective internalization of NPs into lung cancer cells through CD44-mediated endocytosis (where HA binds to the overexpressed CD44 receptors onto cancer cells) followed by glutathione (GSH) stimulus release of GA into the cytoplasm. Flow cytometry and confocal imaging results demonstrate that HA receptors mediate the cellular uptake and burst drug release in the highly reducing cytosol of NPs. HA(HECS-ss-OA)/GA has demonstrated pronounced cytotoxicity and apoptosis against A549 compared to the HA uncoated NPs. In addition, less systemic cytotoxicity was observed in mice treated with HA/chitosan/GA NPs compared to mice treated with free GA.[71] Thus, the HA/chitosan/GA NPs were good candidates for cancer therapy.

Table 4 Nano-hydrogels loaded with gambogic acid for cancer therapy

Type of nanocarrier	Composition	Cancer cell line	Advantages	Ref.
Hydrogel NPs	Hydroxypropyl cellulose, silk fibroin, and glycerol	Gastric cancer MKN-45	- A thermosensitive and injectable hydrogel with a short gelling time - Sustained release	79
Hydrogel NPs	mPEG-PCL micelles (GA-MIC) mixed with poly (D,L-lactide)–poly(ethylene glycol)–poly(D,L-lactide) (PLEL)	Oral squamous cell carcinoma	- A thermosensitive hydrogel - Improved antitumor immune activation - Facilitated the local delivery and sustained release of GA - Reduced the immunosuppressive cellular components	78
Hydrogel NPs	Poly(ethylene glycol) dimethacrylate and sericin methacryloyl	Triple-negative breast cancer	- Sustained release of GA - Activated antitumor immune responses - Inhibited local tumor recurrence	80
Hydrogel NPs	Sodium alginate, 2,2′-azobis [2-(2-imidazolin-2-yl) propane] dihydrochloride (AIPH), and Ink (a photothermal agent)	Colorectal cancer HCT116 cells	- High effective antitumor activity - Increased reactive oxygen species (ROS) - Boosted ferroptosis	81

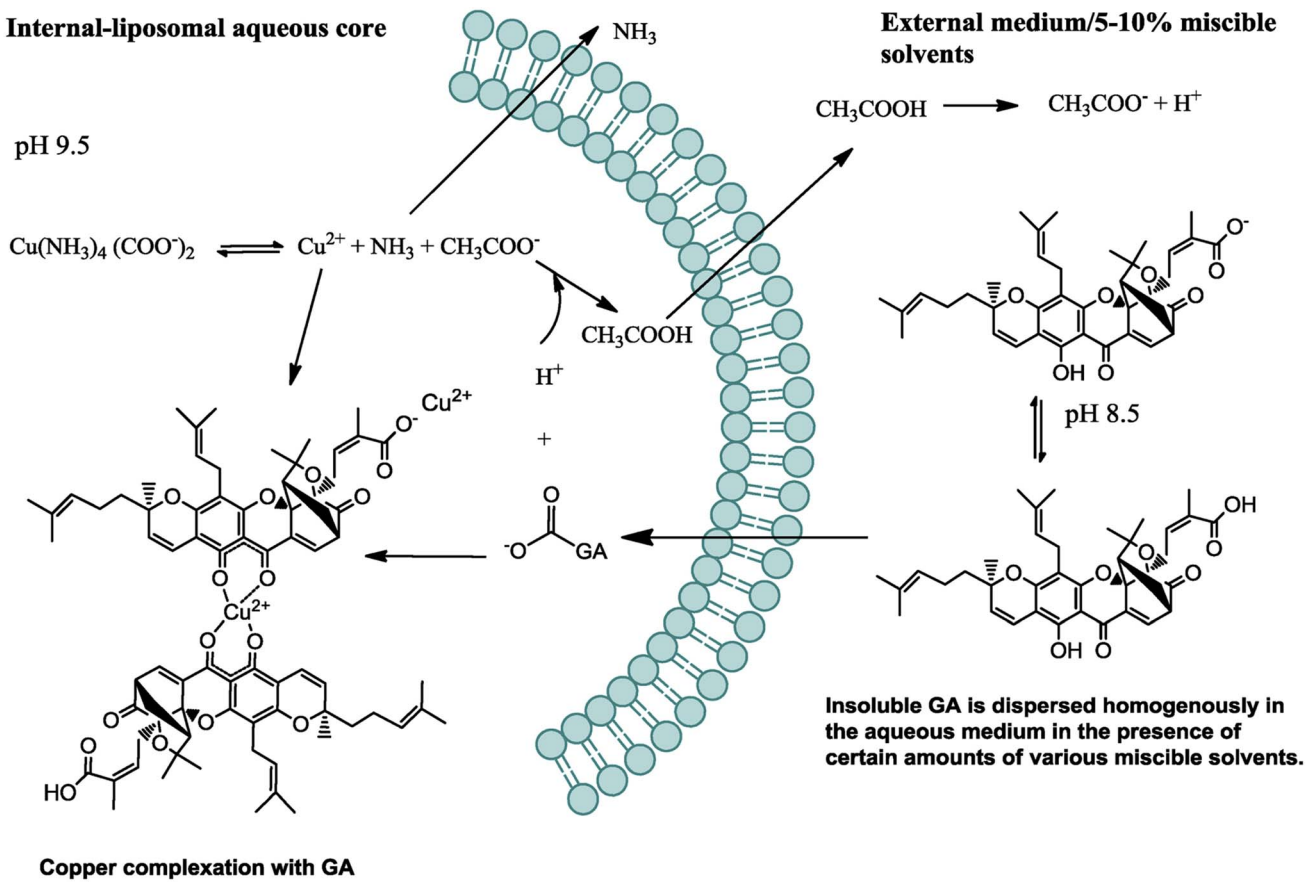

Fig. 10 Schematic diagram depicting the mechanism by which GA was actively loaded inside the nanoliposomes. This figure has been reproduced from ref. 85 with permission from Elsevier, copyright 2018.

A novel study reported the fabrication of biocompatible pH-, esterase- and temperature-sensitive polymeric prodrug of gambogic acid (GA) based on chitosan graftomer for effective cancer therapy. In this regards, folic acid–chitosan conjugates were complexed with thermoresponsive amine-terminated poly-*N*-isopropyl acrylamide (NH_2-PNIPAM), forming FA-CSPN. Then, esterification was involved in coupling GA with the graftomer to attain high drug-entrapment capacity and controlled GA release manner. Finally, the synthesized amphiphilic prodrug, *O*-(gambogic acid)-*N*-(folic acid)-*N*′-(NH_2-PNIPAM) chitosan graftomer (GFCP), was self-assembled forming micelles. The designed nano-micelles have shown enhanced intracellular uptake *via* folate-mediated endocytosis (Fig. 7), followed by the triggered release of GA in the cancer microenvironment. In addition, the micelles showed potent antiproliferation activity and halted tumor growth in H22 tumor-bearing mice while causing no systemic toxicity.[72]

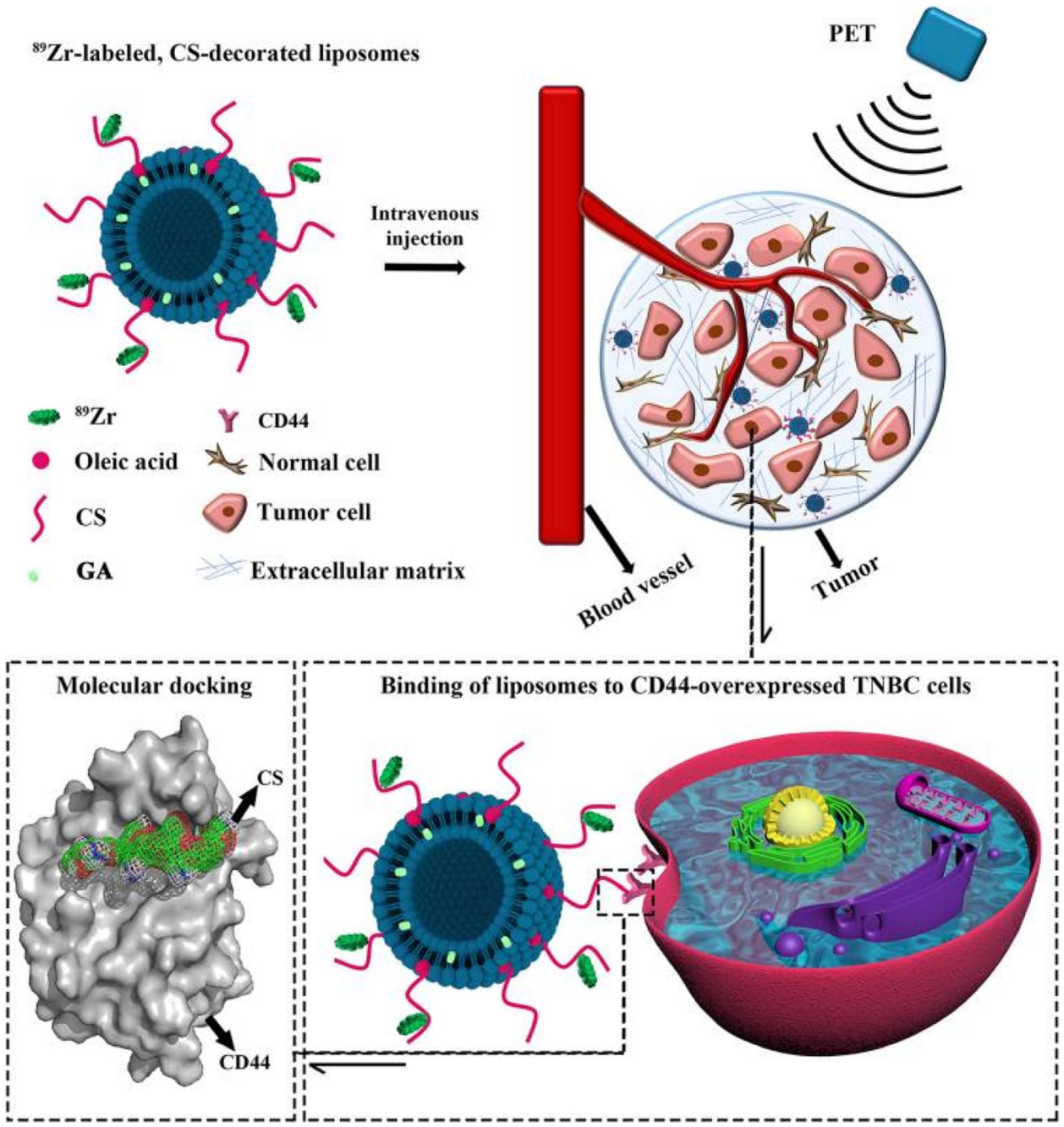

Fig. 11 Schematic diagram illustrating the design of the multifunctional ^{89}Zr-labeled, GA-loaded, CS-decorated liposomes. The biodistribution of designed liposomes was traced by positron emission tomography (PET) imaging, and the binding mechanism was studied by molecular docking. This figure has been reproduced from ref. 87 with permission from Taylor & Francis, 2020.

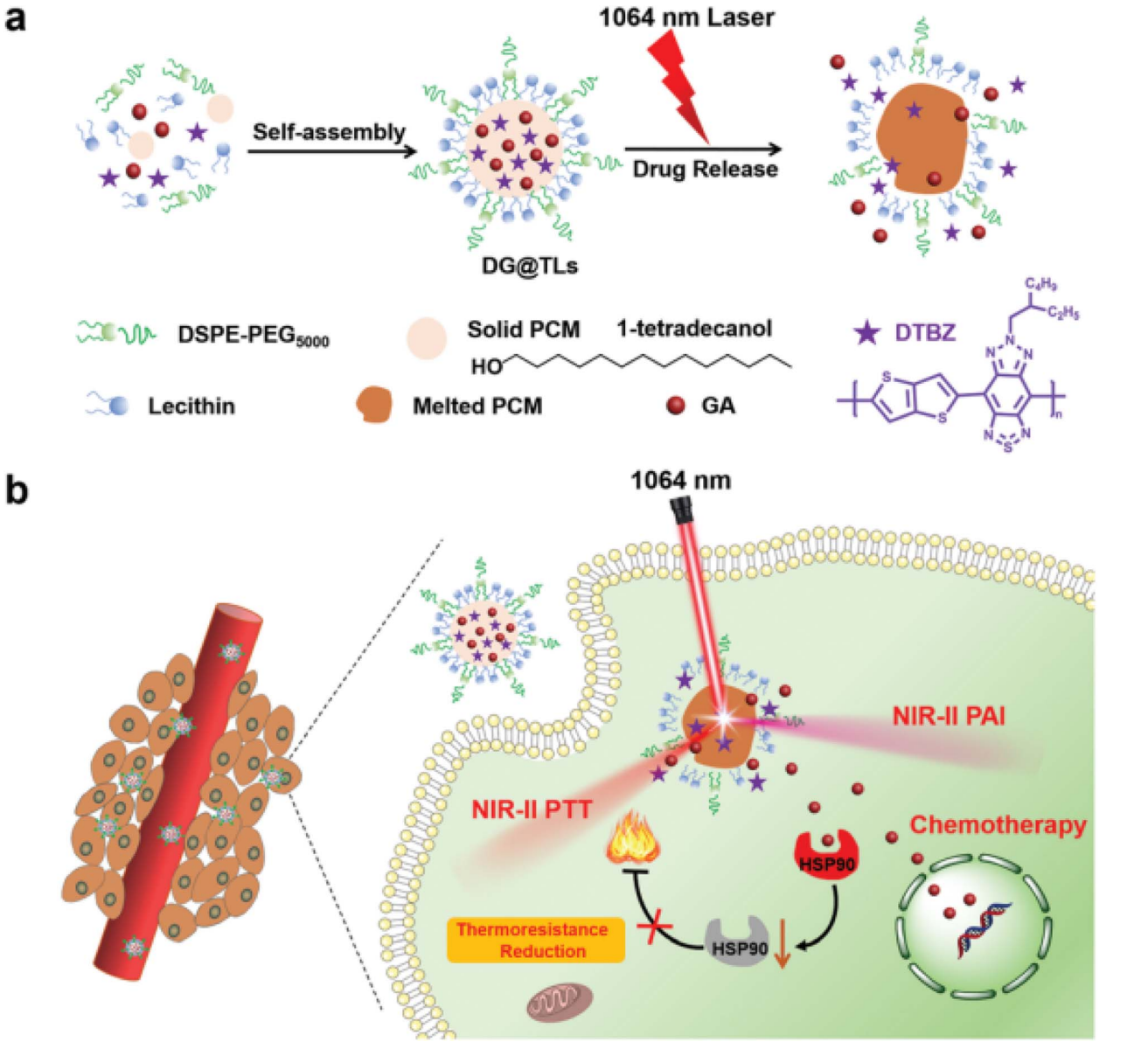

Fig. 12 Schematic diagram illustrating (a) the fabrication of NIR-II light (1064 nm) excitation thermosensitive nano-liposomes (TLs) and (b) the synergistic anticancer effects achieved by the thermo-responsive release of GA causing improved PTT and chemotherapeutic effects against cancers. This figure has been reproduced from ref. 88 with permission from Royal Society of Chemistry, copyright 2022.

Another study reported the synthesis of a copolymer (GPgWSC) formed of a polyethylenimine (PEI)-grafted water-soluble chitosan (WSC) and GA. The fabricated copolymer served as a targeting moiety and transfection augmentation agent. It demonstrated an improved ability to bind the overexpressed transferrin receptors found on the surface of human colon HCT116 cancer cells. Then, GPgWSC was complexed with pDNA (BCL2 shRNA-expressing vector, psiRNA-BCL2) through electrostatic interaction between the cationic WSC/PEI and the anionic pDNA forming nano-sized polyplexes that carry GA on their outer surfaces. The engineered polyplexes were transported inside cancer cells *via* transferrin receptor-mediated endocytosis, followed by endosomal escape owing to the proton sponge effect of PEI, disconnection of polyplexes, movement of pDNA into the nucleus, shRNA expression, and gene silencing (Fig. 8). Due to the apoptotic activity of psiRNA-hBCL2, the nanopolyplexes displayed higher *in vitro* anticancer activity. *In vivo* study revealed that the tumor mass of the HCT116 mouse model treated with saline expanded to 2270 mm^2. On the other hand, those treated with the nano-sized have shown a dramatic decrease in the tumor mass with a size of 248 mm^2.[65]

Table 3 summarizes the studies that involved using polymeric NPs to encapsulate GA.

5.2 Hydrogels

The hydrogel system demonstrated improved anticancer activity in *in vivo* trials and superior biodegradability,

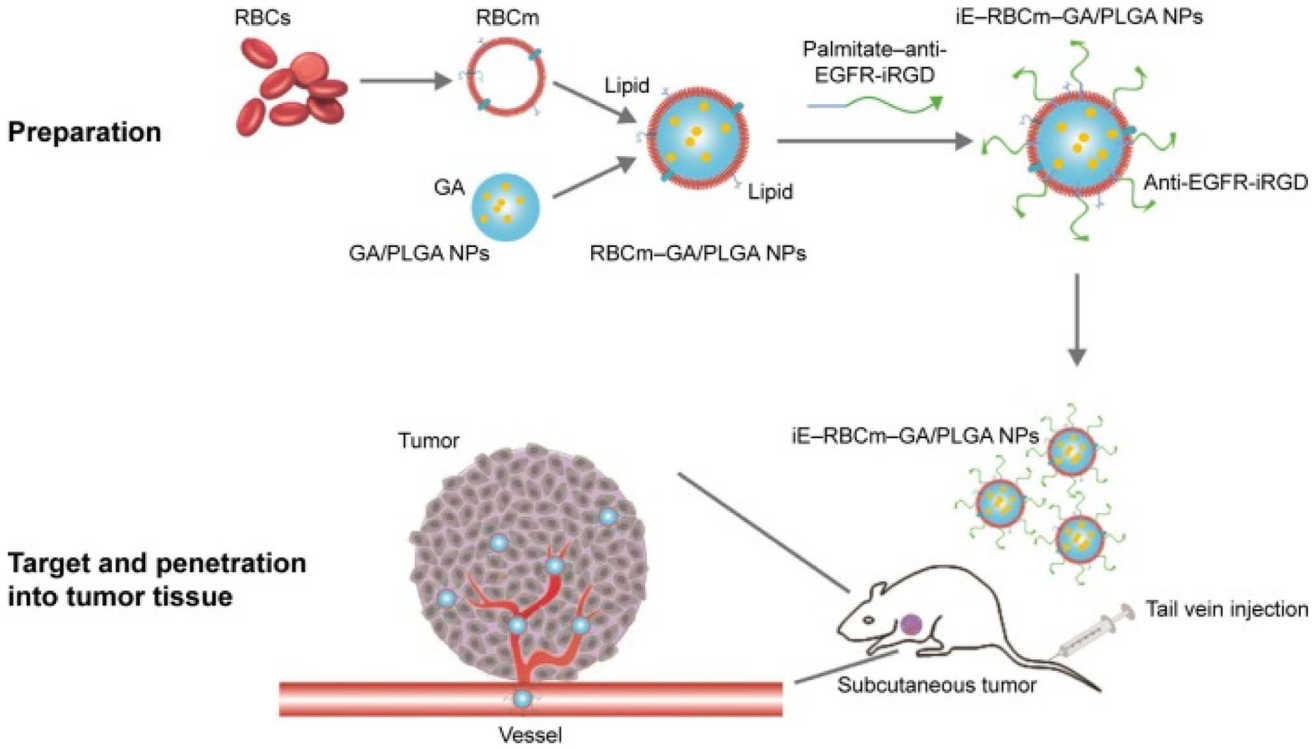

Fig. 13 Schematic illustration of iE-RBCm-GA/PLGA NPs fabrication with improved targeting capacity and antitumor efficiency. This figure has been reproduced from ref. 75 with permission from Taylor & Francis, copyright 2018.

biocompatibility, and low toxicity. Hydrogel nanocarriers are used in cancer treatment due to their superior properties, ability to be used as controlled drug release systems, and capability to achieve a sustained release behavior. Because hydrogel materials come in a variety of sizes and delivery methods, they can be tailored to specific cancer kinds and regions.[77]

A study reported the design of thermosensitive hydrogel loaded with GA for treating oral squamous cell carcinomas (OSCC). In this regards, the aqueous solubility of GA was initially improved by loading it into $mPEG_{2000}$-PCL micelles (GA-MIC) using the thin-film hydration technique. Then, in order to prepare the thermosensitive hydrogel, the prepared GA-MIC was mixed at room temperature with synthesized poly(D,L-lactide)–poly(ethylene glycol)–poly(D,L-lactide) (PLEL) to design a therapeutic hydrogel that could be injected (GA-MIC-GEL), as presented in Fig. 9. It was revealed that the designed GA-MIC-GEL was in a liquid state at room temperature, which instantly transformed into a gel state at 37 °C (body temperature). This facilitates the intratumoral or peritumoral administration by injection, increasing the local concentration of GA and improving the anticancer effect while minimizing the systemic adverse effects of GA. The use of implanted hydrogel for the local delivery of anticancer therapeutic agents is promising for the effective remedy of OSCC and other surface tumors, such as skin and breast tumors. Moreover, the anticancer effect of GA-MIC-GEL was assessed on the mouse squamous cell carcinoma (SCC-7) subcutaneous xenograft mouse model. GA-MIC-GEL exhibited a pronounced antiproliferative effect with an average tumor inhibition rate of 60.5%. In addition, the immunological studies carried out on OSCC cells showed that the prepared GA-MIC-GEL could control tumor immune microenvironment (TIME) by boosting the levels of cytotoxic T cells and the IFN-γ, while diminishing the expression of systemic PD-1 and the components of immunosuppressive cells inside cancer cells.[78]

A similar study reported the fabrication of injectable thermosensitive hydrogel comprised of hydroxypropyl cellulose, silk fibroin, and glycerol co-loaded with water-soluble GA NPs (with an average size of 200 nm, encapsulation efficiency of 57% and drug loading of 9%) and tumor-penetrating peptide iRGD for the effective treatment of stomach cancer. The thermosensitive hydrogel was designed to overcome the shortcomings that hinder the clinical applications of GA non-specific targeting, water insolubility, unintended toxic effects, and uneven biodistribution and pharmacokinetic profiles. The prepared 20% glycerol hydrogel system exhibited a quick gelling time, outstanding biocompatibility, biodegradability, and an *in vivo* sustained release time, where about 20% of GA and 60% of iRGD were released at 96 h. In addition, the presence of iRGD was shown to increase tumor infiltration, improve the permeability and accumulation of the hydrogel into cancer cells and, hence, boosted the anticancer effect of the hydrogel against stomach cancer, as compared to the free GA. Moreover, safety studies have shown no noticeable toxic effects of GA because the local administration of the injectable hydrogels packaging loaded with GA-NPs and iRGD has allowed a high concentration

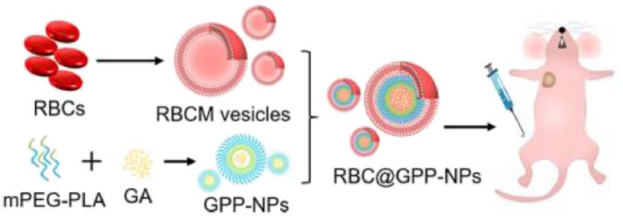

Fig. 14 Schematic representation showing the synthesis of GPP-NPs and coating with RBCM with improved *in vivo* anticancer effect. This figure has been reproduced from ref. 74 with permission from Elsevier, copyright 2023.

of the cargo inside the cancer cells while keeping a reasonably small dose of GA which minimized the systemic toxicity.[79]

The hydrogels involved in the targeted delivery of GA are illustrated in Table 4.

5.3 Nano-liposomes

Nano-liposomes have attracted an increasing interest in the delivery of various anticancer agents, including microRNAs, peptides, chemotherapeutics, and natural compounds. This is attributed to their superb features, such as facile formulation methods, accessibility, biological stability, biocompatibility, and biodegradability. Interestingly, they promote the uptake of their cargo into cancer cells by improving the penetration through the cells, thanks to their structures that resemble the ones found in biological cell membranes.[82–84]

In one study, GA-loaded nanoliposomes were formulated using solvent-assisted active loading technology (SALT). The loading gradient and lipid composition were optimized to create a stable formulation, demonstrating >95% drug retention after being incubated with serum for three days. The optimal loading formulation was based on using basified copper acetate and DOPC/Chol/DSPE-mPEG2K in a molar ratio of 85/10/5, mol%, respectively, as presented in Fig. 10. The permeation of the GA uncharged form into the liposomal core *via* active loading was enhanced using miscible solvents. Then, the GA was ionized and retained inside the liposomal core *via* de-protonation at the basic pH of 9.5. Another factor that prevented the leakage of GA out of the liposomal membranes is its complexation with the cupric ions present in the liposomal core.

Moreover, the designed GA-loaded nano-liposome had an average particle size of 75 nm and a longer circulatory half-life compared to the free GA. Also, it showed an exclusive anticancer mechanism by concurrently downregulating several oncogenes, including NF-kB, Bcl-2, Stat3, HIF-1α, and VEGF-A, resulting in remarkable anti-angiogenesis and antiproliferation activities in the treated tumor with noteworthy tumor relapse.[85]

Another study reported the fabrication of a nano-lactoferrin-modified GA liposomal delivery system to overcome the GA limitations and increase the therapeutic efficacy in colorectal cancer. The designed nanoliposomes showed a high binding capacity to the LRP-1 receptor that is overexpressed on the surface of colorectal cancer cells, leading to an improved selective targeting ability to the cancer cells and, thus, boosted therapeutic efficacy. Moreover, the designed nanoliposomes could repolarize tumor-associated macrophages from the M2 to M1 phenotype and induce ICD to activate T cells, demonstrating the ability to alter the tumor immune microenvironment. Nanoliposomes also increased tumor cell apoptosis and autophagy and decreased tumor cells' reactive oxygen species (ROS) levels.[86]

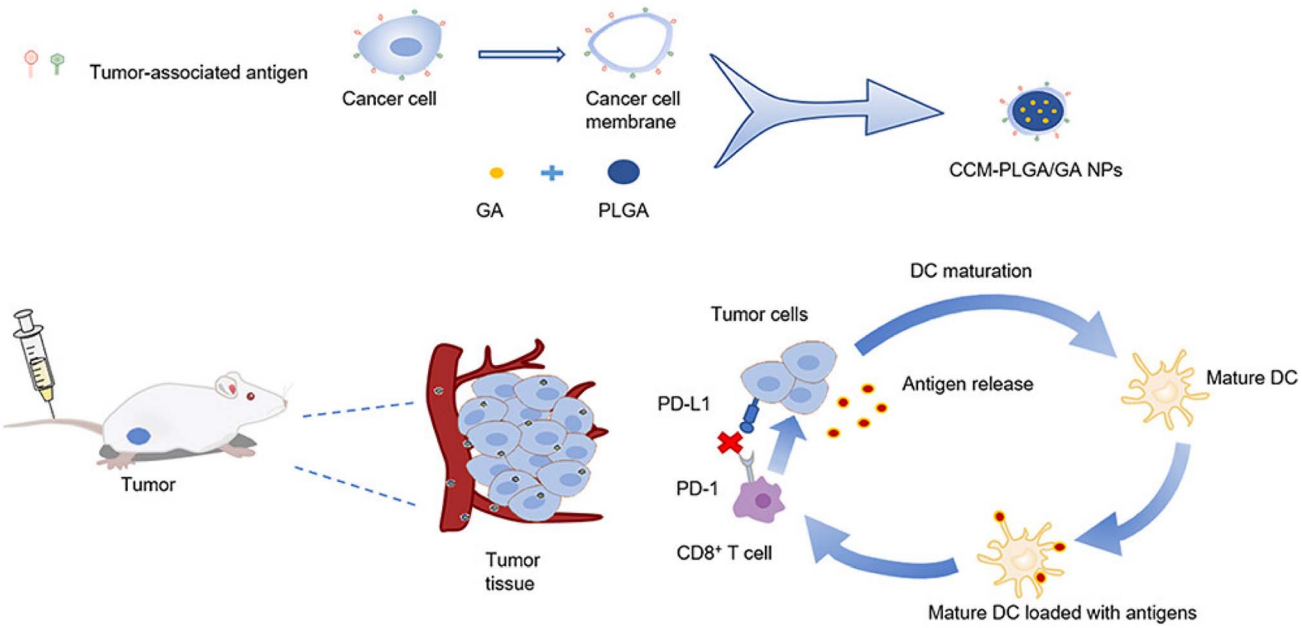

Fig. 15 Illustrative diagram showing the synthesis of CCM-PLGA/GA NPs and its impact on the tumor microenvironment. This figure has been reproduced from ref. 73 with permission from Taylor & Francis, copyright 2023.

A promising study reported the engineering of multifunctional liposomes loaded with GA, surface-functionalized with chitosan (CS), and labeled with zirconium-89 (^{89}Zr) to precisely target and trace cluster of differentiation 44$^+$ (CD44$^+$), which are overexpressed in triple-negative breast cancer (TNBC) stem cells (Fig. 11). Molecular docking and dynamics simulations revealed that CS could be docked into the active site of CD44 in a satisfactory and stable conformation. Moreover, ^{89}Zr@CS-GA-MLPs have shown selective binding to CD44$^+$ TNBC stem-like cells and uptaken into the cancer cells of xenograft-bearing mice with outstanding radiochemical stability. Finally, GA-loaded ^{89}Zr@CS-GA-MLPs exhibited significant antitumor efficiency *in vivo*.[87]

In another recent study, NIR-II light (1064 nm) excitation thermosensitive nano-liposomes (TLs) co-loaded with synthesized semiconducting polymer (thiadiazole benzotriazole (DTBZ)) and GA were designed. The TLs were designed utilizing the resolidification method where the aqueous solution composed of DTBZ, GA, and phase change material (PCM, 1-tetradecanol with a melting point of 38–39 °C) was added dropwise to lipid solution composed of DSPE-PEG5000, lecithin, and, as presented in Fig. 12. DTBZ was incorporated into the TLs to attain strong absorption in the NIR-II region. The TLs were prepared to achieve synergistic anticancer activity against mouse melanoma's highly metastatic cell line B16F10 cells by combining photothermal (PTT) and chemotherapeutic effects. Upon exposure to 1064 nm laser irradiation, TLs displayed robust photoacoustic signals and outstanding photothermal therapy (PTT) efficacy against innate tumors. The activation of the thermos-responsive release of GA relied on the phase transition of PCMs from solid phase to liquid one. The prepared TLs demonstrated improved PTT capability with deep tumor penetration while the phase transition of PCMs from solid phase to liquid one triggered the thermo-responsive release of GA. The released GA diminished the thermo-resistance of cancer cells by impeding the activity of HSP90, leading to an increase in PTT effectiveness and achieving a synergistic anticancer effect through its remarkable chemotherapeutic activity. Thus, this study presents a new approach for achieving on-site drug release and efficient theranostics in deep-rooted complex malignancies.[88]

5.4 Biomimetic nanoparticles, immunotherapy RNAs

Biomimetic nanoparticles are biomaterials embedded into the NPs surface that can simulate real cells' biological

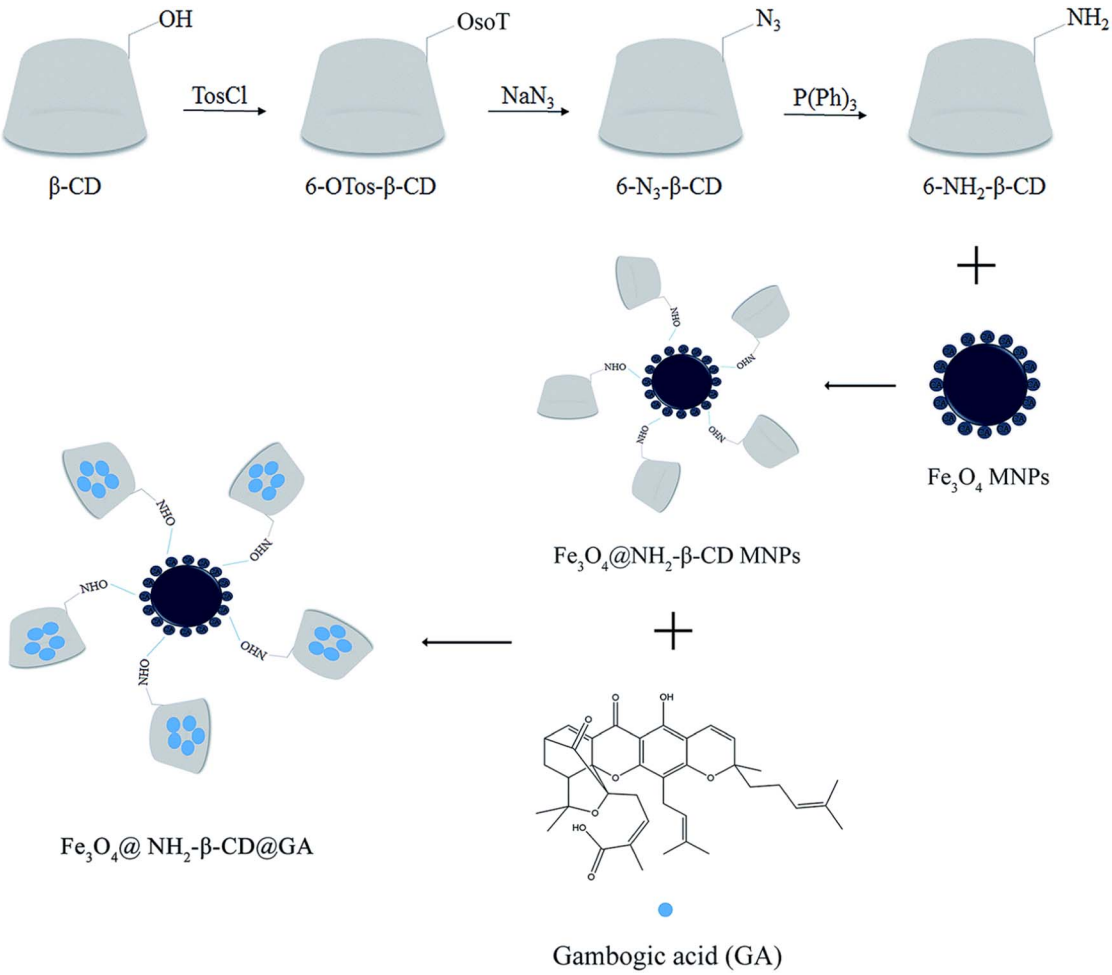

Fig. 16 An illustration depicting the steps involved in the synthesis of Fe_3O_4@NH_2-β-CD@GA MNPs. This figure has been reproduced from ref. 91 with permission from Royal Society of Chemistry, copyright 2019.

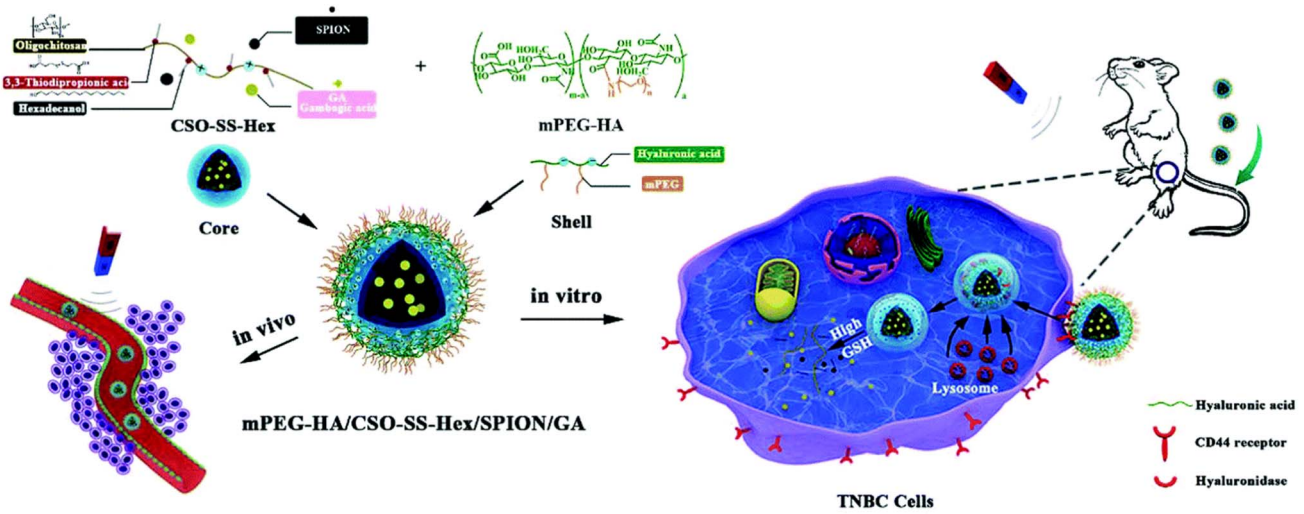

Fig. 17 The preparation of mPEG-HA/CSO-SS-Hex/SPION/GA nanosystem *via* self-assembly. This figure has been reproduced from ref. 92 with permission from Royal Society of Chemistry, copyright 2020.

characteristics and functions. As a result, they have high biocompatibility, advanced targeting specificity, and long retention time. This mimicry method decreases the possibility of hazardous side effects while favoring the escape of biomimetic NPs from immune system clearance. Biomimetic NPs can be coated with various biomaterials to enhance their capacity for biomimicry, including erythrocyte, neutrophil, macrophage, platelet, and cancer cell membranes. As well as synthetic biomaterials like targeting peptides and aptamers, there are biomaterials inspired by nature, including monoclonal antibodies, viral capsids, and natural proteins. It has been demonstrated that NPs coated with red blood cell membrane (RBCm) significantly increased the half-life, mimicking the prolonged circulation period of normal RBCs.[89] For instance, GA was loaded in bispecific targeting biomimetic NPs in one study. In this regards, the anti-EGFR-iRGD recombinant proteins were chemically lipidated using palmitate, adopting the detergent dialysis technique. Then, the lipid chain terminus of palmitate-anti-EGFR-iRGD proteins was inserted onto the lipid bilayered red blood cell (RBC) membranes coating GA loaded PLGA NPs to form RBCm PLGA NPs, using the lipid insertion approach, modified with anti-EGFR-iRGD proteins (iE-RBCm-PLGA NPs), as presented in Fig. 13. Compared to the unmodified RBCm-PLGA NPs, more iE-RBCm-PLGA NPs could be uptaken by colon cancer cells multicellular spheroids (MCS) and exhibited enhanced penetration into MCS *in vitro*. Moreover, iE-RBCm-PLGA NPs also demonstrated better targeting capacity in the *in vivo* nude mice-bearing tumor model of colorectal cancer while showing prominent accumulation at the cancer site. More importantly, the iE-RBCm-GA/PLGA NPs lowered GA systemic toxic effects and warranted *in vivo*.[75]

In another recent study, GA was loaded into mPEG-PLA NPs (GPP-NPs) and then mimicked with the erythrocyte membrane (RBCM) to form RBC@GPP-NPs using the membrane dialysis method (DLS), as shown in Fig. 14. The biomimetic NPs were designed to overcome the drawbacks of GA by improving its hydrophilicity, stability, and safety while boosting its anticancer activity against hepatic cancer cells (HepG2). The average particle sizes of RBC@GPP-NPs and GPP-NPs were narrow, and monodisperse were 102.3 ± 3.1 nm and 89.55 ± 0.92 nm, respectively. This confirmed the successful coating of NPs with RBCM where the size increment equals the thickness of RBCM (about 12 nm). The encapsulation efficiency (EE) of RBC@GPP-NPs and GPP-NPs were 79.11 ± 1.42% and 86.37 ± 0.84%, respectively, representing the efficient loading of GA. Moreover, RBC@GPP-NPs exhibited more potent anticancer activity *in vivo* while warranting the safety of systemic administration.[74]

In a similar study, GA was loaded in PLGA NPs and coated with neoantigen, colon cancer cell membrane CT26 (CCM), forming CCM-PLGA/GA NPs, to be used as a nano-vaccine to enhance the anticancer immune response of colorectal cancer (CRC). The NPs were found to trigger the maturation of dendritic cells (DC), boost the expression of $CD8^+$ T cells in the spleen, and diminish the expression of PD-L1 on tumor cells and PD-1 on $CD8^+$ T cells, suggesting the ability to create a positive tumor immune microenvironment, as presented in Fig. 15. In addition, *in vivo* experiments revealed that coating the PLGA/GA NPs with CCM caused higher concentrations of NPs to escape the immune system phagocytosis, where they penetrated the tumor cells effectively to exert anticancer effects. Thus, the prepared nano-vaccine had promise for clinical application and might warrant a new tactic in the fight against colorectal cancer.[73]

5.5 Inorganic nanocarriers

Inorganic NPs (Fig. 2), such as silica, silver, gold, supramagnetic iron oxide NPs, carbon dots, and quantum dots, have shown great promise in cancer therapy, diagnosis, and imaging. This is attributed to their tailored nano-scale sizes, biological stability, small sizes, ease of functionalization, and outstanding cellular uptake and penetration capacity *via* the passive mode of delivery. However, the clinical application of inorganic Nos remains very challenging due to the potential systemic toxicities

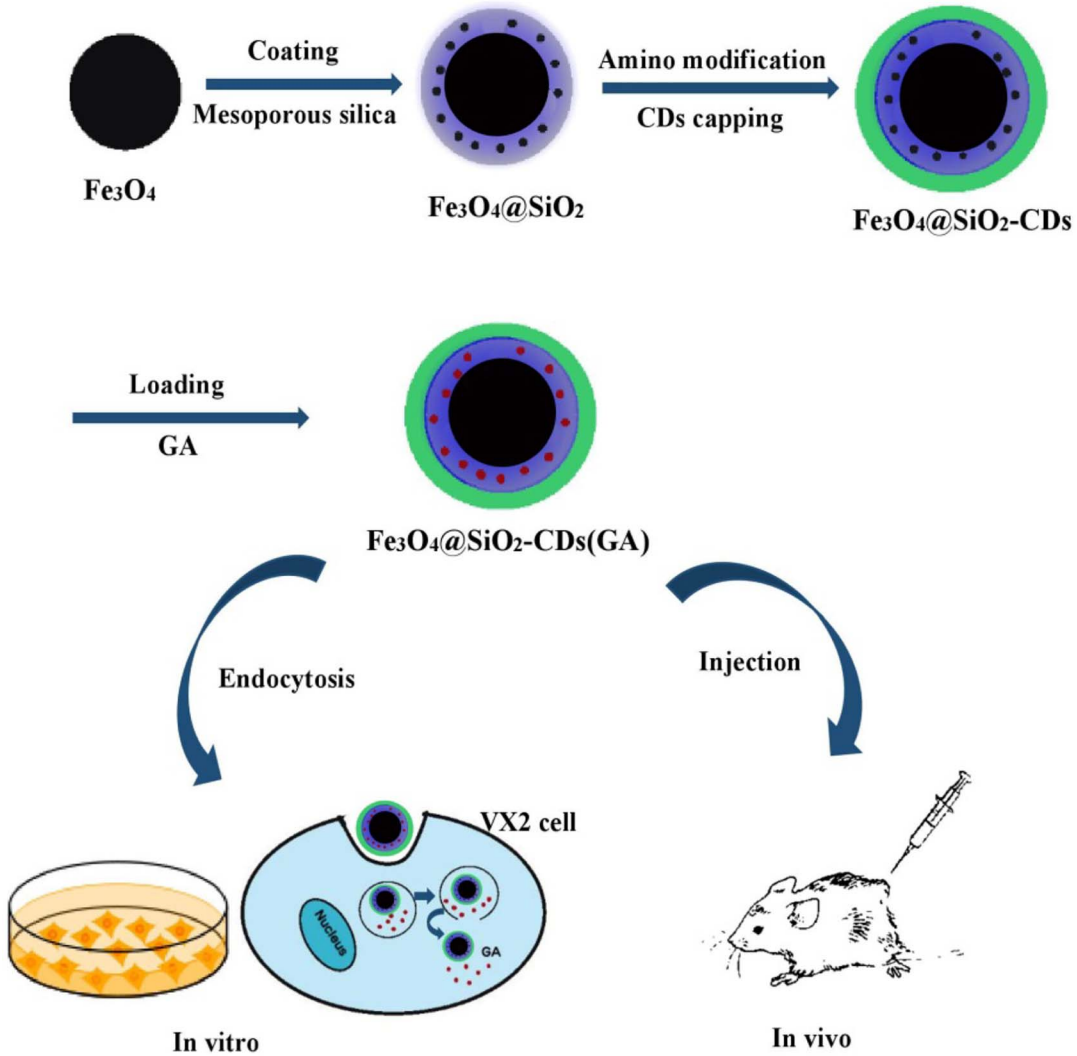

Fig. 18 The fabrication of multifunctional Fe_3O_4@SiO_2-CDs loaded with GA and their targeted uptake into cancer cells *via* endocytosis. This figure has been reproduced from ref. 93 with permission from Elsevier, copyright 2021.

that might be linked with their use.[90] Specifically, supramagnetic Fe_3O_4 NPs have several features, including biocompatibility, high cellular internalization, magnetic resonance, and magnetic hyperthermia properties. Several studies reported the integration of magnetic targeting with chemotherapeutics for synergistic cancer therapy. For instance, in one study, a nano-delivery system based on aminated β-cyclodextrin (6-NH_2-β-CD)-grafted Fe_3O_4 and GA clathrate complexes were synthesized to minimize the GA vascular irritability and improve targeting and bioavailability. As depicted in Fig. 16, 6-NH_2-β-CD was synthesized by reduction reaction where the 6-position hydroxyl group of β-CD was substituted with p-TosCl, NaN_3, and $P(Ph)_3$. Then, EDCI and NHS were used to activate the carboxyl group (on the citric acid) on the surface of Fe_3O_4 to react with ammonia on 6-NH_2-β-CD forming an amide, and generating the host molecule (Fe_3O_4@NH_2-β-CD MNPs). Then, the guest molecule, GA, was included in the host molecule to create the nano complex Fe_3O_4@NH_2-β-CD@GA MNPs. The nanocomplexes had an average particle size of 147.4 ± 0.28 nm and a PDI of 0.072 ± 0.013. In addition, the nanocomplexes had encapsulation efficiency, drug loading, zeta potential, and magnetic saturation values of 85.71 ± 3.47%, 4.63 ± 0.04%, −29.3 ± 0.42 mV, and 46.68 emu g^{-1}, respectively. Moreover, the synthesized nanocomplexes showed augmented cytotoxicity against HL-60 and HepG2 cell lines (0.348 and 0.964 μg mL^{-1}, respectively), as compared to free GA (0.818 μg mL^{-1} and 1.525 μg mL^{-1}, respectively).[91] More importantly, it was revealed that the vascular irritation of GA was diminished upon encapsulation into Fe_3O_4@NH_2-β-CD due to minimizing the direct contact of GA with the vascular endothelium, which warrants its intravenous administration.[91]

Another study reported the engineering of a tumor-targeted redox controllable self-assembled nanosystem loaded with GA with magnetic improved EPR effects (mPEG-HA/CSO-SS-Hex/SPION/GA) to augment the anticancer effectiveness of GA (Fig. 17). The nanosystem was prepared *via* self-assembly and composed of three layers: (i) an exterior layer formed of monoaminated poly(ethylene glycol) grafted hyaluronic acid (mPEG-

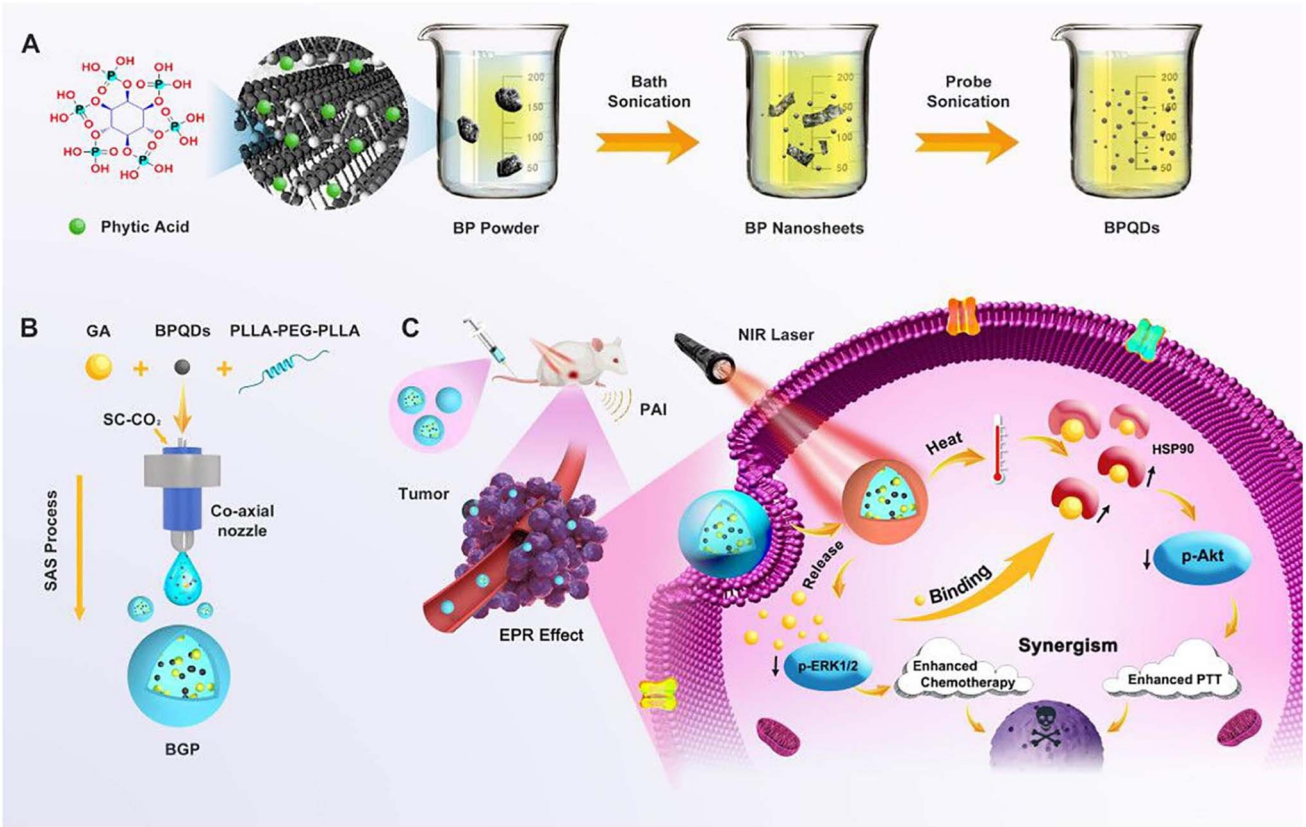

Fig. 19 Depicting the (A) formulation of BPQDs, (B) preparation of BPQDs/GA/PLLA-PEG-PLLA (BGP) nanocomposites, and (C) their synergistic chemo-photothermal therapeutic effects. This figure has been reproduced from ref. 96 with permission from Elsevier, copyright 2020.

HA), which can target the CD44 receptor in TNBC cells, (ii) a middle layer composed of disulfide-linked hexadecanol (Hex) and chitosan oligosaccharide (CSO) to monitor the drug release by redox stimulus effect, (iii) an inner layer formed of super-paramagnetic iron oxide nanoparticles (SPION), which can improve the EPR effect by magnetic guidance and responsible for the encapsulation of GA.[92]

In a different study, a multifunctional platform formed of terminated magnetic mesoporous silica nanoparticles grafted with fluorescent carbon quantum dots (CDs) (Fe_3O_4@SiO_2-CDs) enhanced the synergistic anticancer activity of GA against breast cancer VX2 cells (Fig. 18). Multifunctional magnetic fluorescent nanocomposite particles are created by an amide reaction between high-fluorescent carbon quantum dots (CD) prepared by microwave method and amino-functional Fe_3O_4 and SiO_2 with high saturation magnetic strength and a core–shell structure loaded with GA. The prepared nanoplatform had an average size of 155.0 nm and its saturated magnetization was 31.2 emu/g. In addition, it showed a pH dependent release of GA of 68% at pH 5.7 (simulating timor microenvironment) compared to 35% in physiological pH (pH = 7.4). Confocal laser scanning microscopy and MTT cell showed that Fe_3O_4@SiO_2-CDs were able to penetrate VX2 cells through endocytosis and a cell survival rate lower than 20% at a concentration of 100 μg mL^{-1}. Moreover, *in vivo* study in VX2 tumor-bearing mice showed that the magnetic targeting experimental group had an obvious downward trend, suggesting that the multifunctional magnetic NPs had a robust magnetic targeting capacity on malignancies.[93]

In a similar study, a dual-functional ellipsoidal-Fe_3O_4@-SiO_2@mSiO_2-C_{18}@dopamine hydrochloride-graphene quantum dots-folic acid (ellipsoidal-HMNPs@PDA-GQDs-FA),Fe_3O_4 was loaded with GA was synthesized to improve the anticancer activity of GA against the same cancer cells, VX2 cells. The hydrothermal approach generated the α-Fe_2O_3 ellipsoidal NPs, which were coated with SiO_2 by the Stöber approach. Graphene quantum dots, dopamine hydrochloride, and folic acid were grafted onto the NPs *via* an amide reaction. The formulated NPs with GA had a high loading capacity (51.63 ± 1.53%) and release (38.56 ± 1.95%) for GA. Following GA loading, a significant increase in cell lethality of 74.91 ± 1.2% was observed. This is attributed to the magnetic targeting of NPs and the capacity of folic acid to escort NPs to the tumor microenvironment. After loading GA, all results demonstrated that the NPs had acceptable biocompatibility and could be used to treat VX2 tumor cells.[94]

Another reported work presented the fabrication of Fe_3O_4/hydrophilic mesoporous silica NPs hollow spheres as a drug carrier (HMNPs). Then, polyethyleneimine (PEI) and N- and S-doped graphene quantum dots (NS-GQDs) were attached to the surface of HMNPs. Finally, two targeting moieties, hyaluronic acid (HA) and folic acid (FA), decorated the surfaces of the hollow nanospheres, forming HMNPs-NS-GQDs-PEI-HA and

HMNPs-NS-GQDs-PEI-FA nanocomposites, respectively, which could be uptaken by VX2 cancer cells for fluorescence confocal imaging. The designed smart nanocomposites enhanced the photoluminescence activity of GQDs and created conjugated quantum dots with GA, leading to a synergistic intelligent enhancement of the GA efficiency. The two nanocomposites exhibited good biocompatibility, minimal cytotoxicity, high GA loading capacity, and pH-responsive drug release behavior. In addition, after 24 h, the cell survival rates of HMNPs-NS-GQDs-PEI-HA and HMNPs-NS-GQDs-PEI-FA encapsulating GA were 7.69% and 8.71%, respectively. *In vivo* assessment showed that the nanocomposites could inhibit tumor proliferation and had magnetic targeting ability.[95]

In a recent study, poly(L-lactide)–poly(ethylene glycol)–poly(L-lactide) triblock copolymer (PLLA–PEG–PLLA)-based nanocomposites co-encapsulated with black phosphorus quantum dots (BPQDs) and GA employing the supercritical carbon dioxide approach (Fig. 19). In this regards, BPQDs were synthesized utilizing a liquid exfoliation method involving probe ultrasonication. Then, the synthesized BPQDs and GA were entrapped into PLLA–PEG–PLLA copolymer employing the supercritical anti-solvent approach, creating BPQDs/GA/PLLA–PEG–PLLA (BGP) nanocomposites. Distinctive PT and an NIR-stimulated release of GA characterize the formulated nanocomposites. More importantly, the fabricated nanocomposites reduced the thermoresistance of cancer by downregulating the overexpressed HSP90 by the incorporated GA cells, augmenting the sensitization of the cancer cells to photothermal ablation. Moreover, the synthesized nanocomposites were shown to have strong apoptotic effects by curbing the expression of anti-apoptotic p-ERK1/2 and p-Akt.[96]

5.6 Combination therapy of nano-chemotherapy with GA

The clinical applicability of the combination therapy involving GA and other chemotherapeutics is hindered by the difficulty of

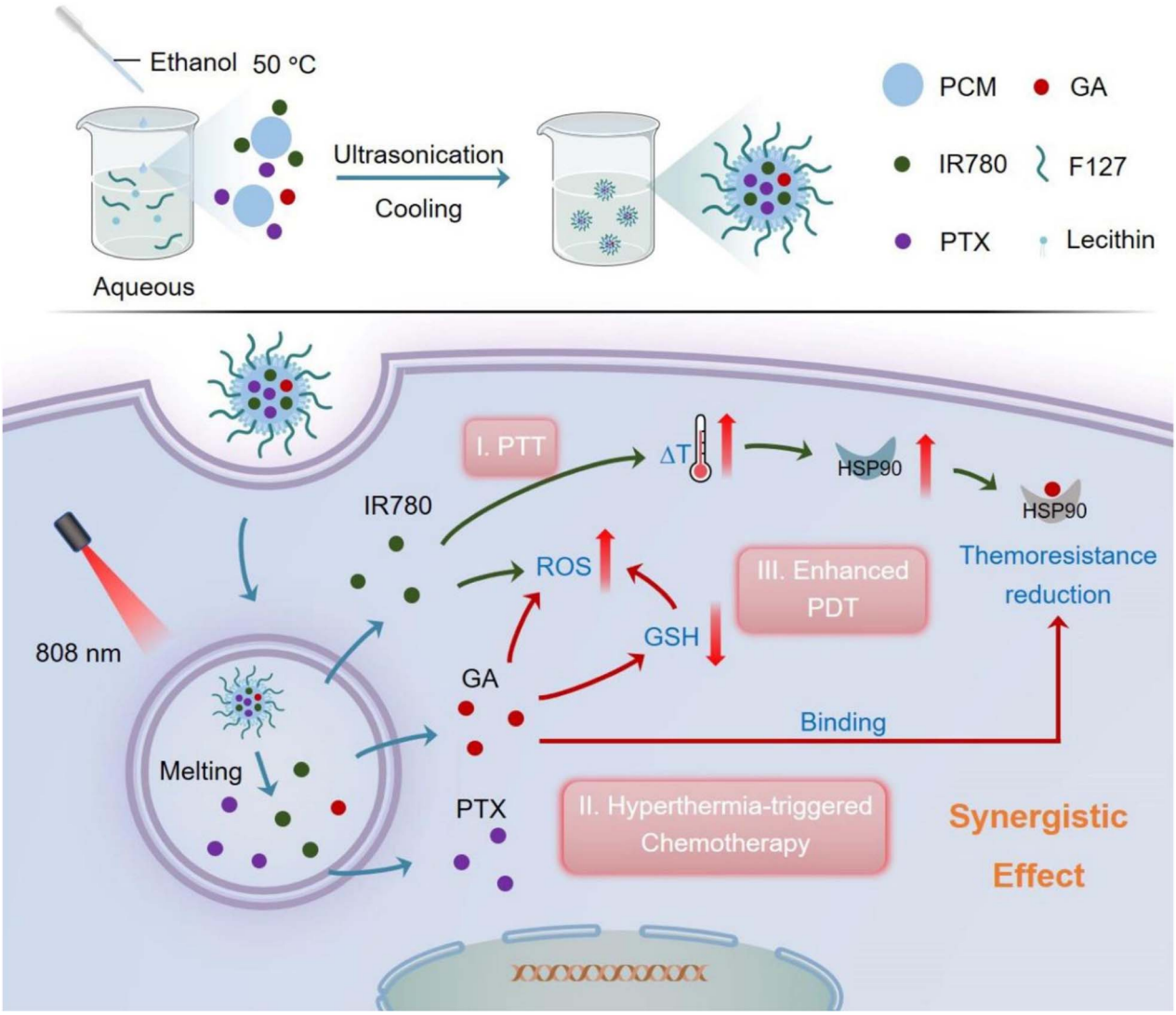

Fig. 20 A schematic diagram summarizing the design of PTX-IR780-GA NPs and their synergistic mechanism in ablating breast cancer. This figure has been reproduced from ref. 98 with permission from Elsevier, copyright 2023.

determining the proper dosage regimen, therapeutic outcome, patient compliance, GA water insolubility, and severe toxic effects. In addition, combinational therapies suffer from altered pharmacokinetic and pharmacodynamic characteristics and poor biodistribution.[97] Based on these factors, the nanodrug delivery systems can significantly improve the circulation lifetime, pharmacokinetic constraints, and internalization of combined drugs into the tumor. In one study, GA and doxorubicin (DOX) were co-loaded into bovine serum albumin (BSA) nanoparticles. The dual-loaded NPs exhibited a synergistic effect in halting HepG2 tumor cells at a combination index (CI) of 0.38, demonstrating substantial synergism by CI < 0.7. In addition, the *ex vivo* fluorescence imaging assessment showed high internalization of GA and DOX into cancer cells owing to the EPR effect, which boosted the fabricated NPs' anticancer effect. Significantly, the synergistic *in vivo* antitumor efficiency is attained at a 3-fold lower combined treatment dose than the single treatment.[97]

Another study reported the formulation of a novel phase change material (PCM)-based nanosystem co-loaded with paclitaxel (PTX), IR780 and GA was developed by ultrasonication approach for the dually-boosted phototherapy of breast cancer. When exposed to NIR illumination, the dually loaded NPs showed an IC50 value of at 5.5 ng mL^{-1}, suggesting a superb synergistic therapeutic effectiveness against breast cancer cells. The NPs were uptaken into the cancer cells *via* the EPR effect, then upon exposure to laser illumination, IR780 generated ROS and mild hyperthermia, resulting in PTT and PDT effects. In addition, hyperthermia was essential to trigger the transition of PCM from the solid phase to the liquid one, thus releasing the co-loaded PTX and GA for dual-improvement of photo/chemotherapies and minimizing the systemic toxic effects. Moreover, as mentioned earlier, GA impeded the overexpression of HSP90 to reduce the thermal resistance of tumor cells. In addition, GA depleted the GSH stores inside the cancer cells and, thus, improved intracellular ROS content, which improved the effectiveness of PDT (Fig. 20). To this end, this novel nanosystem showed great potential in concurrently overcoming serious challenges by advancing the effectiveness of synergistic photo/chemo/photodynamic therapies.[98]

6. Conclusion and future perspectives

Despite being a promising natural compound in cancer treatment, GA suffers several limitations that impede its clinical translation. Among these limitations are water-insolubility, biological instability, low oral bioavailability, poor pharmacokinetic and biodistribution profiles, vascular irritation, and non-selective selective targeting of tumor tissues. This review presented the latest state-of-the-art studies describing the nanoformulation of GA into various organic, inorganic and hybrid nanodelivery systems. Several studies reported using nanodelivery systems in cancer-targeted therapies due to their unorthodox capabilities to modernize cancer therapeutics by extending the circulation time of their cargos, enhancing bioavailability and water solubility while minimizing detrimental toxic effects. Moreover, escorting therapeutic agents by different nanodelivery particulates can selectively augment their accumulation into tumor tissues by passive targeting. Despite the attempts to develop safe and biocompatible nanosystems that encapsulate GA alone or in combination with other therapeutic agents, the clinical application of NPs is still challenging. This is attributed to the unscalable invention method and complicated drug pharmacokinetics and pharmacodynamics in the body. In addition, the NPs might endure drug leakage, resulting in low drug loading and encapsulation efficiencies. Moreover, there is scarce information on the *in vivo* absorption, distribution, metabolism, elimination routes, and immunological reactions of the different nanoparticles. Forthcoming work should examine the biosafety and pharmacodynamics interests concerned with applying nanosystems in cancer remedies instead of focusing only on their fabrication, chemical functionalization, and *in vitro* applications. This will provide a prosperity of information to unveil the safest and most targetable nanocarrier that would be the hallmark for inventing more advanced cancer therapies. Moreover, future work should provide more comprehensive immunological assessments to study the GA immune regulation mechanisms on different cancer cells.

Conflicts of interest

There are no conflicts to declare.

References

1 N. K. Sedky, *et al.*, Box–Behnken design of thermo-responsive nano-liposomes loaded with a platinum(IV) anticancer complex: evaluation of cytotoxicity and apoptotic pathways in triple negative breast cancer cells, *Nanoscale Adv.*, 2023, **5**(19), 5399–5413.
2 I. Ritacco, *et al.*, Hydrolysis in acidic environment and degradation of satraplatin: a joint experimental and theoretical investigation, *Inorg. Chem.*, 2017, **56**(10), 6013–6026.
3 H. M. E.-S. Azzazy, *et al.*, Peganum harmala Alkaloids and Tannic Acid Encapsulated in PAMAM Dendrimers: Improved Anticancer Activities as Compared to Doxorubicin, *ACS Appl. Polym. Mater.*, 2022, **4**(10), 7228–7239.
4 S. A. Fahmy, *et al.*, Thermosensitive Liposomes Encapsulating Nedaplatin and Picoplatin Demonstrate Enhanced Cytotoxicity against Breast Cancer Cells, *ACS Omega*, 2022, **7**(46), 42115–42125.
5 N. K. Sedky, *et al.*, Nedaplatin/Peganum harmala Alkaloids Co-Loaded Electrospun, Implantable Nanofibers: A Chemopreventive Nano-Delivery System for Treating and Preventing Breast Cancer Recurrence after Tumorectomy, *Pharmaceutics*, 2023, **15**(10), 2367.
6 S. A. Fahmy, *et al.*, Synthesis, characterization and host–guest complexation of asplatin: improved *in vitro*

cytotoxicity and biocompatibility as compared to cisplatin, *Pharmaceuticals*, 2022, **15**(2), 259.

7 R. A. Youness, *et al.*, Oral Delivery of Psoralidin by Mucoadhesive Surface-Modified Bilosomes Showed Boosted Apoptotic and Necrotic Effects against Breast and Lung Cancer Cells, *Polymers*, 2023, **15**(6), 1464.

8 S. A. Fahmy, *et al.*, Ozonated Olive Oil: Enhanced Cutaneous Delivery *via* Niosomal Nanovesicles for Melanoma Treatment, *Antioxidants*, 2022, **11**(7), 1318.

9 N. K. Sedky, *et al.*, Co-Delivery of Ylang Ylang Oil of Cananga odorata and Oxaliplatin Using Intelligent pH-Sensitive Lipid-Based Nanovesicles for the Effective Treatment of Triple-Negative Breast Cancer, *Int. J. Mol. Sci.*, 2023, **24**(9), 8392.

10 S. A. Fahmy, *et al.*, Green extraction of essential oils from *Pistacia lentiscus* resins: encapsulation into Niosomes showed improved preferential cytotoxic and apoptotic effects against breast and ovarian cancer cells, *J. Drug Delivery Sci. Technol.*, 2023, **87**, 104820.

11 H. M. E.-S. Azzazy, *et al.*, Essential Oils Extracted from Boswellia sacra Oleo Gum Resin Loaded into PLGA–PCL Nanoparticles: Enhanced Cytotoxic and Apoptotic Effects against Breast Cancer Cells, *ACS Omega*, 2022, **8**(1), 1017–1025.

12 D. A. Dias, S. Urban and U. Roessner, A historical overview of natural products in drug discovery, *Metabolites*, 2012, **2**(2), 303–336.

13 S. Nobili, *et al.*, Natural compounds for cancer treatment and prevention, *Pharmacol. Res.*, 2009, **59**(6), 365–378.

14 E. Hatami, *et al.*, Gambogic acid potentiates gemcitabine induced anticancer activity in non-small cell lung cancer, *Eur. J. Pharmacol.*, 2020, **888**, 173486.

15 K. Na, *et al.*, A solvent-assisted active loading technology to prepare gambogic acid and all-trans retinoic acid co-encapsulated liposomes for synergistic anticancer therapy, *Drug Delivery Transl. Res.*, 2020, **10**, 146–158.

16 E. Hatami, *et al.*, Gambogic acid: a shining natural compound to nanomedicine for cancer therapeutics, *Biochim. Biophys. Acta*, 2020, **1874**(1), 188381.

17 M. Sharma, *et al.*, Cancer treatment and toxicity outlook of nanoparticles, *Environ. Res.*, 2023, **237**, 116870.

18 R. T. Attia, *et al.*, Newly Synthesized Anticancer Purine Derivatives Inhibiting p-EIF4E Using Surface-Modified Lipid Nanovesicles, *ACS Omega*, 2023, **8**(41), 37864–37881.

19 F. Ponte, *et al.*, Psoralidin–cucurbit [7] uril complex with improved solubility to tackle human colorectal cancer: experimental and computational study, *Mater. Adv.*, 2023, **4**(21), 5324–5337.

20 Q.-B. Han, *et al.*, Stability and cytotoxicity of gambogic acid and its derivative, gambogoic acid, *Biol. Pharm. Bull.*, 2005, **28**(12), 2335–2337.

21 C. Wen, *et al.*, Gambogic acid inhibits growth, induces apoptosis, and overcomes drug resistance in human colorectal cancer cells, *Int. J. Oncol.*, 2015, **47**(5), 1663–1671.

22 J. Chen, *et al.*, Microtubule depolymerization and phosphorylation of c-Jun N-terminal kinase-1 and p38 were involved in gambogic acid induced cell cycle arrest and apoptosis in human breast carcinoma MCF-7 cells, *Life Sci.*, 2008, **83**(3–4), 103–109.

23 R. Li, *et al.*, Gambogic acid induces G0/G1 arrest and apoptosis involving inhibition of SRC-3 and inactivation of Akt pathway in K562 leukemia cells, *Toxicology*, 2009, **262**(2), 98–105.

24 J. Wang, *et al.*, Studies on chemical structure modification and biology of a natural product, Gambogic acid (I): Synthesis and biological evaluation of oxidized analogues of gambogic acid, *Eur. J. Med. Chem.*, 2009, **44**(6), 2611–2620.

25 J. Yang, *et al.*, Gambogic acid deactivates cytosolic and mitochondrial thioredoxins by covalent binding to the functional domain, *J. Nat. Prod.*, 2012, **75**(6), 1108–1116.

26 Y.-Y. Wang, *et al.*, Progress in research of the structural optimization of natural product-like Garcinia caged xanthones, *Acta Pharm. Sin. B*, 2014, **49**(3), 293–302.

27 R.-T. Li, *et al.*, Synergistic photothermal-photodynamic-chemotherapy toward breast cancer based on a liposome-coated core–shell AuNS@ NMOFs nanocomposite encapsulated with gambogic acid, *J. Nanobiotechnol.*, 2022, **20**(1), 1–22.

28 R. Verma, *et al.*, Evaluation of methotrexate encapsulated polymeric nanocarrier for breast cancer treatment, *Colloids Surf., B*, 2023, **226**, 113308.

29 S. y. Jiang, *et al.*, Gambogic acid inhibits epithelial–mesenchymal transition in breast cancer cells through upregulation of SIRT1 expression *in vitro*, *Precis. Med. Sci.*, 2022, **11**(1), 14–22.

30 Y. Wang, Y. Sui and Y. Tao, Gambogic acid increases the sensitivity to paclitaxel in drug-resistant triple-negative breast cancer *via* the SHH signaling pathway, *Mol. Med. Rep.*, 2019, **20**(5), 4515–4522.

31 X. Li, *et al.*, Involvement of E-cadherin/AMPK/mTOR axis in LKB1-induced sensitivity of non-small cell lung cancer to gambogic acid, *Biochem. Pharmacol.*, 2019, **169**, 113635.

32 D. Lin, *et al.*, Gambogic acid inhibits the progression of gastric cancer *via* circRNA_ASAP2/miR-33a-5p/CDK7 axis, *Cancer Manage. Res.*, 2020, **12**, 9221–9233.

33 Z. Joha, *et al.*, Mechanism of anticancer effect of gambogic acid on gastric signet ring cell carcinoma, *Med. Oncol.*, 2023, **40**(9), 269.

34 R. Yapasert and R. Banjerdpongchai, Gambogic Acid and Piperine Synergistically Induce Apoptosis in Human Cholangiocarcinoma Cell *via* Caspase and Mitochondria-Mediated Pathway, *J. Evidence-Based Complementary Altern. Med.*, 2022, 6288742.

35 K. Suksen, *et al.*, Gambogic acid inhibits wnt/β-catenin signaling and induces ER stress-mediated apoptosis in human cholangiocarcinoma, *Asian Pac. J. Cancer Prev.*, 2021, **22**(6), 1913.

36 D. Duan, *et al.*, Gambogic acid induces apoptosis in hepatocellular carcinoma SMMC-7721 cells by targeting cytosolic thioredoxin reductase, *Free Radicals Biol. Med.*, 2014, **69**, 15–25.

37 H. Xu, *et al.*, Gambogic acid induces pyroptosis of colorectal cancer cells through the GSDME-dependent pathway and

elicits an antitumor immune response, *Cancers*, 2022, **14**(22), 5505.
38 X. Wang, *et al.*, Effect of gambogic acid on miR-199a-3p expression and cell biological behavior in colorectal cancer cells, *J. Oncol.*, 2021, **2021**, 5140621.
39 Z. Zhou and J. Ma, Gambogic acid suppresses colon cancer cell activity *in vitro*, *Exp. Ther. Med.*, 2019, **18**(4), 2917–2923.
40 G.-M. Huang, *et al.*, Gambogic acid induces apoptosis and inhibits colorectal tumor growth *via* mitochondrial pathways, *World J. Gastroenterol.*, 2015, **21**(20), 6194.
41 G. Gao, *et al.*, Gambogic acid regulates the migration and invasion of colorectal cancer *via* microRNA-21-mediated activation of phosphatase and tensin homolog, *Exp. Ther. Med.*, 2018, **16**(3), 1758–1765.
42 Y.-Z. Zhen, *et al.*, Gambogic acid lysinate induces apoptosis in breast cancer mcf-7 cells by increasing reactive oxygen species, *J. Evidence-Based Complementary Altern. Med.*, 2015, **2015**, 842091.
43 Z. Zou, *et al.*, Synergistic anti-proliferative effects of gambogic acid with docetaxel in gastrointestinal cancer cell lines, *BMC Complementary Altern. Med.*, 2012, **12**(1), 1–9.
44 H. Wang, *et al.*, Gambogic acid induces autophagy and combines synergistically with chloroquine to suppress pancreatic cancer by increasing the accumulation of reactive oxygen species, *Cancer Cell Int.*, 2019, **19**, 1–15.
45 L. Wang, *et al.*, Gambogic acid synergistically potentiates cisplatin-induced apoptosis in non-small-cell lung cancer through suppressing NF-κB and MAPK/HO-1 signalling, *Br. J. Cancer*, 2014, **110**(2), 341–352.
46 X. Shi, *et al.*, Gambogic acid induces apoptosis in imatinib-resistant chronic myeloid leukemia cells *via* inducing proteasome inhibition and caspase-dependent Bcr-Abl downregulation, *Clin. Cancer Res.*, 2014, **20**(1), 151–163.
47 Y. Kang, *et al.*, Redox-responsive polymeric micelles formed by conjugating gambogic acid with bioreducible poly(amido amine)s for the co-delivery of docetaxel and MMP-9 shRNA, *Acta Biomater.*, 2018, **68**, 137–153.
48 J. Wei, *et al.*, Gambogic acid potentiates the chemosensitivity of colorectal cancer cells to 5-fluorouracil by inhibiting proliferation and inducing apoptosis, *Exp. Ther. Med.*, 2017, **13**(2), 662–668.
49 T. Ren, *et al.*, Gambogic acid suppresses nasopharyngeal carcinoma *via* rewiring molecular network of cancer malignancy and immunosurveillance, *Biomed. Pharmacother.*, 2022, **150**, 113012.
50 L. Liu, *et al.*, Nanomedicine-based combination of gambogic acid and retinoic acid chlorochalcone for enhanced anticancer efficacy in osteosarcoma, *Biomed. Pharmacother.*, 2016, **83**, 79–84.
51 R. Ning, *et al.*, Gambogic acid potentiates clopidogrel-induced apoptosis and attenuates irinotecan-induced apoptosis through down-regulating human carboxylesterase 1 and-2, *Xenobiotica*, 2016, **46**(9), 816–824.
52 C. Wang, *et al.*, Combined therapy with EGFR TKI and gambogic acid for overcoming resistance in EGFR-T790M mutant lung cancer, *Oncol. Lett.*, 2015, **10**(4), 2063–2066.
53 J. Huang, *et al.*, Combined effects of low-dose gambogic acid and NaI 131 in drug-resistant non-small cell lung cancer cells, *Oncol. Lett.*, 2021, **22**(2), 1–8.
54 J. Conniot, *et al.*, Cancer immunotherapy: nanodelivery approaches for immune cell targeting and tracking, *Front. Chem.*, 2014, **2**, 105.
55 T. Briolay, *et al.*, Delivery of cancer therapies by synthetic and bio-inspired nanovectors, *Mol. Cancer*, 2021, **20**, 1–24.
56 I. Arshad, *et al.*, Effect of hydrophilic and hydrophobic polymer on the release of ketoprofen and allopurinol from bilayer matrix transdermal patch, *Adv. Polym. Technol.*, 2018, **37**(8), 3076–3083.
57 A. M. Ayoub, *et al.*, Photodynamic and antiangiogenic activities of parietin liposomes in triple negative breast cancer, *Biomater. Adv.*, 2022, **134**, 112543.
58 A. A. Dayyih, *et al.*, Thermoresponsive Liposomes for Photo-Triggered Release of Hypericin Cyclodextrin Inclusion Complex for Efficient Antimicrobial Photodynamic Therapy, *ACS Appl. Mater. Interfaces*, 2022, **14**(28), 31525–31540.
59 S. Biswas, *et al.*, Recent advances in polymeric micelles for anti-cancer drug delivery, *Eur. J. Pharm. Sci.*, 2016, **83**, 184–202.
60 M. Shabbir, *et al.*, Influence of different formulation variables on the performance of transdermal drug delivery system containing tizanidine hydrochloride: *in vitro* and *ex vivo* evaluations, *Braz. J. Pharm. Sci.*, 2019, **54**, e00130.
61 M. Y. Ali, *et al.*, Selective anti-ErbB3 aptamer modified sorafenib microparticles: *in vitro* and *in vivo* toxicity assessment, *Eur. J. Pharm. Biopharm.*, 2019, **145**, 42–53.
62 L. Cai, *et al.*, Improving aqueous solubility and antitumor effects by nanosized gambogic acid-mPEG2000 micelles, *Int. J. Nanomed.*, 2014, 243–255.
63 S. Ali, *et al.*, Lipoparticles for synergistic chemo-photodynamic therapy to ovarian carcinoma cells: *in vitro* and *in vivo* assessments, *Int. J. Nanomed.*, 2021, 951–976.
64 M. U. Amin, *et al.*, Co-delivery of carbonic anhydrase IX inhibitor and doxorubicin as a promising approach to address hypoxia-induced chemoresistance, *Drug Delivery*, 2022, **29**(1), 2072–2085.
65 S.-C. Park, H. Heo and M.-K. Jang, Polyethylenimine grafted-chitosan based gambogic acid copolymers for targeting cancer cells overexpressing transferrin receptors, *Carbohydr. Polym.*, 2022, **277**, 118755.
66 A. Behl, *et al.*, Biodegradable diblock copolymeric PEG-PCL nanoparticles: synthesis, characterization and applications as anticancer drug delivery agents, *Polymer*, 2020, **207**, 122901.
67 K. Song, *et al.*, A novel dual sensitive polymer-gambogic acid conjugate: synthesis, characterization, and *in vitro* evaluation, *Nanotechnology*, 2019, **30**(50), 505701.
68 W. Zhu, *et al.*, Construction of long circulating and deep tumor penetrating gambogic acid-hydroxyethyl starch nanoparticles, *J. Drug Delivery Sci. Technol.*, 2022, **77**, 103910.
69 D. Zhang, *et al.*, Gambogic acid-loaded PEG–PCL nanoparticles act as an effective antitumor agent against gastric cancer, *Pharm. Dev. Technol.*, 2018, **23**(1), 33–40.

70 F. Wang, *et al.*, Ultrasound-triggered drug delivery for glioma therapy through gambogic acid-loaded nanobubble-microbubble complexes, *Biomed. Pharmacother.*, 2022, **150**, 113042.
71 W. Xu, *et al.*, Hyaluronic acid-decorated redox-sensitive chitosan micelles for tumor-specific intracellular delivery of gambogic acid, *Int. J. Nanomed.*, 2019, 4649–4666.
72 Q. Du, *et al.*, A multiple environment-sensitive prodrug nanomicelle strategy based on chitosan graftomer for enhanced tumor therapy of gambogic acid, *Carbohydr. Polym.*, 2021, **267**, 118229.
73 F. Huang, *et al.*, Cancer Cell Membrane-Coated Gambogic Acid Nanoparticles for Effective Anticancer Vaccination by Activating Dendritic Cells, *Int. J. Nanomed.*, 2023, 2261–2273.
74 R. Liu, *et al.*, Erythrocyte membrane encapsulated gambogic acid nanoparticles as a therapeutic for hepatocellular carcinoma, *Chin. Chem. Lett.*, 2023, **34**(1), 107575.
75 Z. Zhang, *et al.*, Anti-EGFR-iRGD recombinant protein modified biomimetic nanoparticles loaded with gambogic acid to enhance targeting and antitumor ability in colorectal cancer treatment, *Int. J. Nanomed.*, 2018, 4961–4975.
76 X. Xu, *et al.*, Mucoadhesive nanoparticles based on ROS activated gambogic acid prodrug for safe and efficient intravesical instillation chemotherapy of bladder cancer, *J. Controlled Release*, 2020, **324**, 493–504.
77 X. Li, *et al.*, Hydrogel systems for targeted cancer therapy, *Front. Bioeng. Biotechnol.*, 2023, **11**, 1140436.
78 X. Chen, *et al.*, Local delivery of gambogic acid to improve anti-tumor immunity against oral squamous cell carcinoma, *J. Controlled Release*, 2022, **351**, 381–393.
79 D. Zhang, *et al.*, Antitumor activity of thermosensitive hydrogels packaging gambogic acid nanoparticles and tumor-penetrating peptide iRGD against gastric cancer, *Int. J. Nanomed.*, 2020, 735–747.
80 D. Mi, *et al.*, Postsurgical wound management and prevention of triple-negative breast cancer recurrence with a pryoptosis-inducing, photopolymerizable hydrogel, *J. Controlled Release*, 2023, **356**, 205–218.
81 X. Su, *et al.*, Localized disruption of redox homeostasis boosting ferroptosis of tumor by hydrogel delivery system, *Mater. Today Bio*, 2021, **12**, 100154.
82 R. Kumar, A. Singh and N. Garg, Acoustic cavitation-assisted formulation of solid lipid nanoparticles using different stabilizers, *ACS Omega*, 2019, **4**(8), 13360–13370.
83 R. Kumar, *et al.*, Preparation, characterization and *in vitro* cytotoxicity of Fenofibrate and Nabumetone loaded solid lipid nanoparticles, *Mater. Sci. Eng., C*, 2020, **106**, 110184.
84 S. El-Shafie, *et al.*, Encapsulation of nedaplatin in novel pegylated liposomes increases its cytotoxicity and genotoxicity against a549 and U2OS human cancer cells, *Pharmaceutics*, 2020, **12**(9), 863.
85 W.-L. Tang, *et al.*, Systemic study of solvent-assisted active loading of gambogic acid into liposomes and its formulation optimization for improved delivery, *Biomaterials*, 2018, **166**, 13–26.
86 R. Wang, *et al.*, Lactoferrin-Modified Gambogic Acid Liposomes for Colorectal Cancer Treatment, *Mol. Pharm.*, 2023, **20**(8), 3925–3936.
87 R. Yang, *et al.*, 89Zr-Labeled multifunctional liposomes conjugate chitosan for PET-trackable triple-negative breast cancer stem cell targeted therapy, *Int. J. Nanomed.*, 2020, 9061–9074.
88 Y. Dai, *et al.*, Near-infrared-II light excitation thermosensitive liposomes for photoacoustic imaging-guided enhanced photothermal-chemo synergistic tumor therapy, *Biomater. Sci.*, 2022, **10**(2), 435–443.
89 C. Y. Beh, *et al.*, Advances in biomimetic nanoparticles for targeted cancer therapy and diagnosis, *Molecules*, 2021, **26**(16), 5052.
90 P. Chowdhury, *et al.*, Magnetic nanoformulations for prostate cancer, *Drug discovery today*, 2017, **22**(8), 1233–1241.
91 W. Fang, *et al.*, Aminated β-cyclodextrin-grafted Fe_3O_4-loaded gambogic acid magnetic nanoparticles: preparation, characterization, and biological evaluation, *RSC Adv.*, 2019, **9**(47), 27136–27146.
92 M. Sang, *et al.*, CD44 targeted redox-triggered self-assembly with magnetic enhanced EPR effects for effective amplification of gambogic acid to treat triple-negative breast cancer, *Biomater. Sci.*, 2020, **8**(1), 212–223.
93 Y. Guan, *et al.*, Multifunctional Fe_3O_4@SiO_2-CDs magnetic fluorescent nanoparticles as effective carrier of gambogic acid for inhibiting VX2 tumor cells, *J. Mol. Liq.*, 2021, **327**, 114783.
94 M. Dong, *et al.*, Load and release of gambogic acid *via* dual-target ellipsoidal-Fe_3O_4@SiO_2@mSiO_2-C_{18}@dopamine hydrochloride-graphene quantum dots-folic acid and its inhibition to VX2 tumor cells, *Nanotechnology*, 2022, **34**(10), 105101.
95 Z. Chang, *et al.*, Dual-targeting magnetic fluorescent mesoporous organosilicon hollow nanospheres for gambogic acid loading, sustained release and anti-tumor properties, *J. Mol. Liq.*, 2022, **360**, 119412.
96 B.-Q. Chen, *et al.*, Gambogic acid augments black phosphorus quantum dots (BPQDs)-based synergistic chemo-photothermal therapy through downregulating heat shock protein expression, *Chem. Eng. J.*, 2020, **390**, 124312.
97 Z. Chen, *et al.*, Synergistic antitumor efficacy of doxorubicin and gambogic acid-encapsulated albumin nanocomposites, *Colloids Surf., B*, 2020, **196**, 111286.
98 Y. Wang, *et al.*, Dually enhanced phototherapy by gambogic acid and hyperthemia-activated chemotherapy for synergistic breast cancer treatment, *Chem. Eng. J.*, 2023, **452**, 139108.